

# On the infrared behavior of Landau gauge Yang-Mills theory

Christian S. Fischer,<sup>1,2</sup> Axel Maas,<sup>3</sup> and Jan M. Pawłowski<sup>4</sup>

<sup>1</sup>*Institut für Kernphysik, Technische Universität Darmstadt, Schlossgartenstraße 9, D-64289 Darmstadt, Germany*

<sup>2</sup>*GSI Helmholtzzentrum für Schwerionenforschung GmbH, Planckstr. 1 D-64291 Darmstadt, Germany.*

<sup>3</sup>*Institut für Physik, Karl-Franzens Universität Graz, Universitätsplatz 5, A-8010 Graz, Austria.*

<sup>4</sup>*Institut für Theoretische Physik, University of Heidelberg, Philosophenweg 16, D-62910 Heidelberg, Germany.*

(Dated: November 26, 2024)

We discuss the properties of ghost and gluon propagators in the deep infrared momentum region of Landau gauge Yang-Mills theory. Within the framework of Dyson-Schwinger equations and the functional renormalization group we demonstrate that it is only a matter of infrared boundary conditions whether infrared scaling or decoupling occurs. We argue that the second possibility is at odds with global BRST symmetry in the confining phase. For this purpose we improve upon existing truncation schemes in particular with respect to transversality and renormalization.

PACS numbers: 12.38.Aw, 12.38.Lg, 12.38.Gc

## I. INTRODUCTION

In the past decade much progress has been made in the understanding of the infrared sector of QCD described in terms of Green's functions. Various methods have been employed for this purpose, in particular Dyson-Schwinger equations (DSEs) [1, 2, 3, 4, 5, 6, 7, 8, 9, 10, 11, 12, 13, 14, 15, 16, 17, 18, 19, 20, 21], functional Renormalization group equations (FRGs) [10, 22, 23, 24, 25, 26, 27, 28, 29, 30, 31, 32, 33, 34], stochastic quantization methods [35, 36], effective theory approaches [37, 38, 39, 40], and lattice gauge theory [41, 42, 43, 44, 45, 46, 47, 48, 49, 50, 51, 52]. However, as the full Green's functions are non-perturbative, their determination is notoriously complicated, and each and every method faces individual technical problems.

Already in pure Yang-Mills theory the determination of these Green's functions poses a considerable challenge. It is complicated by the fact that these are in general gauge-dependent quantities. However, this fact can also be used to simplify matters by an appropriate choice of gauge. Most commonly Landau gauge has been used in this respect.

Over the past ten years substantial progress has been made using functional methods in this gauge. Based on the pioneering works ref. [1, 4, 36] powerful tools have been developed to analyze the whole tower of Dyson-Schwinger and functional renormalization-group equations in the deep infrared [6, 10]. As a result a self-consistent scenario has been identified which consists of a dressed ghost propagator more divergent in the infrared than its tree-level counterpart and an infrared suppressed gluon propagator with a finite or even vanishing dressing function at zero momentum. This solution agrees well and in fact supports the Kugo-Ojima confinement scenario developed in ref. [53]. As we shall argue below this solution is the only one that has this property.

In lattice gauge theory substantial progress has been made in the past years to overcome intrinsic problems

related to discretization and volume artefacts as well as gauge fixing ambiguities. Recent results on very large volumes [46, 47, 49] produce an infrared finite gluon propagator and, more important, an infrared finite ghost in disagreement with the continuum results discussed above. However, the situation on the lattice is still not settled yet. These results are affected from discretization artefacts [54] and effects due to Gribov copies [43, 48, 55, 56], to a significant extent. We will discuss these issues below in section VII.

Nevertheless, the lattice results have inspired a number of recent works in the continuum theory aiming at solutions of Dyson-Schwinger equations with a finite ghost in the infrared [17, 20, 38]. In this work we confirm that these solutions are present if the functional equations are taken on their own correctly. However, as we will argue in section II B, these solutions cannot represent the infrared behavior of Yang-Mills theory in the confined phase while at the same time maintaining global color symmetry and BRST symmetry.

This work is organized as follows. We will discuss the basic setting, the non-perturbative regime of Yang-Mills theory, and one set of methods to determine these Green's functions, functional equations including boundary conditions, in section II. In particular, in section II B we will discuss the roles of global symmetries and identify boundary conditions necessary to obtain a BRST-symmetric, confining solution. The derivation of the functional equations requires a discussion of certain formal aspects, renormalization and gauge invariance done in section III. In section IV we then discuss the impact of the boundary conditions on the infrared behavior of the ghost and gluon propagators, the simplest Green's functions. As an example we reconsider a truncation scheme for the DSEs which has been introduced in [5]. For the ghost DSE this truncation is identical to those chosen by Boucaud et al. [20] and Aguilar et al. [17]. We also introduce a modified scheme which maintains transversality in the gluon DSE and is free of quadratic divergencies.

We solve the coupled system of ghost and gluon DSEs with different choices of boundary conditions and verify the appearance of two different types of solutions in the infrared. We compare our approach with others and comment on various technical issues. In section VI we repeat this exercise in the framework of the functional renormalization group. We compare and comment on recent lattice results in section VII. We also discuss in section II and VII the role of different non-perturbative extensions of the Landau gauge. In addition, we show in section VIII also that neither type of solution can be associated with a massive gluon characterized by a gauge-independent pole mass. Finally, in section IX we summarize and discuss our results further, the main result being an understanding of how and why both types of solutions exist, and, in the framework of local quantum field theory, which could be the preferred one.

## II. NON-PERTURBATIVE YANG-MILLS THEORY

### A. Gauge-fixing

The starting point for the derivation of functional equations is the gauge-fixed path-integral. Here we shall use Landau gauge,

$$\partial_\mu A_\mu^a = 0. \quad (1)$$

Within the standard Faddeev-Popov gauge fixing procedure this leads to the gauge fixed action in Euclidean space-time

$$S = \int d^d x (F_{\mu\nu}^a F_{\mu\nu}^a + \bar{c}^a \partial_\mu D_\mu^{ab} c^b), \quad (2)$$

with the ghost fields  $\bar{c}^a$  and  $c^a$  and

$$\begin{aligned} F_{\mu\nu}^a &= \partial_\mu A_\nu^a - \partial_\nu A_\mu^a + g f^{abc} A_\mu^b A_\nu^c \\ D_\mu^{ab} &= \delta^{ab} \partial_\mu + g f^{acb} A_\mu^c. \end{aligned} \quad (3)$$

This procedure is only well-defined within perturbation theory. In general there are several gauge equivalent configurations satisfying the gauge condition (1). These are called Gribov copies [57, 58]. Indeed, the related path integral vanishes identically, as contributions from different gauge copies cancel out [59].

The latter problem can be resolved by restricting the configuration space to the first Gribov region [57]. This region is characterized by the condition that the Faddeev-Popov operator  $M^{ab} = -\partial_\mu D_\mu^{ab}$  is positive semi-definite. This gauge prescription is called minimal Landau gauge. However, it is still not sufficient to single out a unique gauge copy [61]. Furthermore it breaks global BRST-invariance, since global BRST transformations relate different Gribov copies [59].

A unique selection of gauge copies can be achieved by restricting the configuration space to the fundamental modular region. This region is characterized by the

global minimum of the gauge fixing potential [61],

$$\mathcal{F}(\mathcal{A}) = c \int d^d x A_\mu^a A_\mu^a, \quad (4)$$

with  $c$  a positive constant. The corresponding gauge is also called the absolute Landau gauge [56]. Based on the work [35] one may hope that absolute Landau gauge is compatible with global BRST symmetry in the thermodynamic limit. This gauge is discussed further in section VII.

### B. Global symmetries and confinement

The appearance of Gribov copies is related to the local (i.e. perturbative) nature of the standard Faddeev-Popov procedure without the supplemental condition of minimising (4). Consequently, to obtain a well-defined non-perturbative functional integral, it is necessary to improve upon this procedure.

A promising approach in this respect is to upgrade the gauge fixing procedure to a globally defined (i.e. non-perturbative) BRST-symmetry that admits global BRST-charges. Then, the path integral is non-vanishing and well-defined. This is also necessary for a successful implementation of BRST symmetry on the lattice [59]. Contrary to the perturbative setting such a procedure implies a weighting of Gribov copies such that the contributions from different gauge copies do not cancel out. Very recently within the framework of topological field theories a globally valid BRST quantisation has been put forward in Ref. [60].

Functional methods such as Dyson-Schwinger or functional Renormalization Group equations have the advantage that such an explicit construction of a gauge fixing in terms of a topological field theory can be avoided. The reason is that global constraints from the gauge fixing procedure do not alter the form of the functional equations but constrain the boundary conditions of Green's functions at vanishing momenta in the infrared. The related infrared constraint has been deduced by consistency arguments for a local covariant quantum field theory, see [4]. This constraint is directly related to the global BRST-charge: the Kugo-Ojima confinement scenario is based on a formulation with well-defined global BRST-charges [53]. These enable the definition of the physical part  $\mathcal{H}_{phys}$  of the state space of Yang-Mills theory in terms of the cohomology of the BRST charge operator and is the basis of the well-known BRST-quartet mechanism. Given furthermore that one is interested in a confining solution of infrared Yang-Mills theory a well-defined global color charge is then necessary to ensure that  $\mathcal{H}_{phys}$  contains only colorless states. In Landau gauge this enforces an infrared enhancement of the ghost propagator [53]; the ghost dressing function is then infrared divergent.

In functional methods this enhancement can be implemented as an infrared renormalization condition. This

condition leads to a unique [10] (scaling) solution of the whole tower of functional equations for the one-particle irreducible Green's functions of Yang-Mills theory. Hence it implicitly defines the unique gauge fixing with well-defined global BRST-charges.

In turn, given confinement, an infrared solution with finite ghost at zero momentum (termed 'decoupling' below) implies broken global gauge and BRST symmetries. Indeed, all known BRST-quantizations that are compatible with an infrared finite ghost even break off-shell BRST [38, 40, 62]. The only possibility for the decoupling solution to coexist with a globally well-defined BRST charge is in a Higgs phase, where the breaking of global color symmetry implies the existence of superselection sectors.

Hence, in the continuum we have a unique scenario with global BRST-charges and an infrared enhanced ghost. These global constraints supplementing Landau gauge are most easily implemented within functional methods with consistent renormalization conditions fixed in the infrared, as will be demonstrated in detail in section IV.

### C. Functional relations

We proceed by briefly discussing the functional relations for the Green's functions we use in the present work following [10].

A quantum field theory or statistical theory can be defined uniquely in terms of its renormalized correlation functions. They are generated by the effective action  $\Gamma$ , the generating functional of 1PI Green's functions. For the functional RG equation we also consider the effective action in the presence of an additional scale  $k$ , where the propagation is modified via  $k$ -dependent terms

$$\Delta S_k = \frac{1}{2} \int A_a^\mu R_{\mu\nu}^{ab} A_b^\nu + \int \bar{C}_a R^{ab} C_b, \quad (5)$$

where  $R_{\mu\nu}^{ab}$  and  $R^{ab}$  are  $k$ -dependent regulator functions. Within the standard choice  $k$  is an infrared cut-off scale, and the functions  $R$  cut-off the propagation for momenta smaller than  $k$ . The regularized effective action  $\Gamma_k$  is expanded in gluonic and ghost vertex functions and reads schematically

$$\Gamma_k[\phi] = \sum_{m,n} \frac{1}{m!n!^2} \Gamma_k^{(2n,m)} \bar{C}^m C^n A^m, \quad (6)$$

in an expansion about vanishing fields  $\phi = (A, C, \bar{C})$ . In (6) an integration over momenta and a summation over indices is understood. The effective action  $\Gamma_k$  satisfies functional relations such as the quantum equations of motion, the Dyson-Schwinger equations (DSEs); symmetry relations, the Ward or Slavnov-Taylor identities (STIs); as well as functional RG or flow equations (FRGs). All these different equations relate to each other, for a detailed discussion see [24]. Indeed, the Slavnov-Taylor

identities are projections of the quantum equations of motion, whereas flow equations can be read as differential DSEs, or DSEs as integrated flows. Written as a functional relation for the effective action  $\Gamma_k$  the DSE reads, *e.g.* [24],

$$\frac{\delta \Gamma_k}{\delta \phi}[\phi] = \frac{\delta S_{\text{cl}}}{\delta \phi}[\phi_{\text{op}}], \quad (7)$$

where the operators  $\phi_{\text{op}}$  are defined as

$$\phi_{\text{op}}(x) = \int d^4y G_{\phi\phi_i}[\phi](x,y) \frac{\delta}{\delta \phi_i(y)} + \phi(x),$$

and

$$G_{\phi_1\phi_2}[\phi] = \left( \frac{1}{\Gamma_k^{(2)}[\phi] + R_k} \right)_{\phi_1\phi_2} \quad (8)$$

is the full field dependent propagator for a propagation from  $\phi_1$  to  $\phi_2$ . The functional derivatives in (7) act on the corresponding fields and generate one loop and two loop diagrams in full propagators. The functional DSE (7) relates 1PI vertices, the expansion coefficients of  $\Gamma_k$ , to a set of one loop and two loop diagrams with full propagators and full vertices, but one classical vertex coming from the derivatives of  $S_{\text{cl}}$ . We emphasize that the DSE (7) only implicitly depends on the regularization via the definition of the propagator in (8).

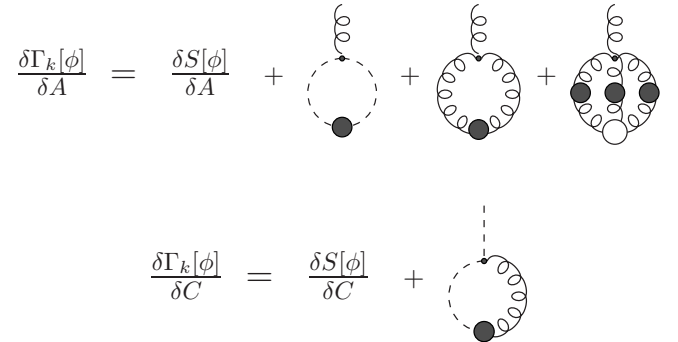


FIG. 1: Functional DSE for the effective action. Filled circles denote fully dressed field dependent propagators (8). Empty circles denote fully dressed field dependent vertices, dots denote field dependent bare vertices.

For Yang-Mills theory a diagrammatic representation of the structure of the functional DSE (7) is shown in Fig. 1. The rhs is given in powers of the field-dependent fully dressed propagator  $G_{\phi\phi}[\phi]$ , and its derivatives, as well as the field dependent bare vertices. The momentum scaling of Green's functions is directly related to the scaling of these building blocks.

Wetterich's flow equation [22] for the effective action of pure Yang-Mills theory reads, *e.g.* [24, 28, 29, 31, 32],

$$\partial_t \Gamma_k[\phi] = \frac{1}{2} \int \frac{d^4p}{(2\pi)^4} G_{ab}^{\mu\nu}[\phi](p,p) \partial_t R_{\mu\nu}^{ba}(p) - \int \frac{d^4p}{(2\pi)^4} G_{ab}[\phi](p,p) \partial_t R^{ba}(p), \quad (9)$$

where  $t = \ln k$ . The flow (9) relates the cut-off scale derivative of the effective action to one loop diagrams with fully dressed field-dependent propagators. We can contrast the diagrammatic representation of the DSE in Fig. 1 with that of (9), given in Fig. 2.

$$\partial_t \Gamma_k[\phi] = \frac{1}{2} \text{ (loop diagram)} - \text{ (loop diagram with cross)}$$

FIG. 2: Functional flow for the effective action. Filled circles denote fully dressed field dependent propagators (8). Crosses denote the regulator insertion  $\partial_t R$ .

Fig. 2 shows the structure of the functional flow (9). The rhs is given by the field-dependent fully dressed propagator  $G_{\phi\phi}[\phi]$  and the regulator insertion  $\partial_t R$ . The standard use of (9) is to take a regulator function  $R(p^2)$  which tends towards a constant in the infrared and decays sufficiently fast in the ultraviolet, and hence implements an infrared cut-off.

$$\begin{aligned} \text{ (loop diagram)}^{-1} &= \text{ (loop diagram)}^{-1} - \frac{1}{2} \text{ (loop diagram)} \\ &- \frac{1}{2} \text{ (loop diagram)} - \frac{1}{6} \text{ (loop diagram)} \\ &- \frac{1}{2} \text{ (loop diagram)} + \text{ (loop diagram)} \\ \text{ (loop diagram)}^{-1} &= \text{ (loop diagram)}^{-1} + \text{ (loop diagram)} \end{aligned}$$

FIG. 3: Dyson-Schwinger equations for the gluon and ghost propagator. Filled circles denote dressed propagators and empty circles denote dressed vertex functions.

The diagrammatical expressions for the exact Dyson-Schwinger equations (DSEs) for the ghost and gluon propagators is given in Fig. 3. The related FRG equations for the propagators are displayed in Fig. 4. The vertices again satisfy DSE/FRG equations which contain vertex functions with a larger number of external legs and so on. Thus in practice, solving DSEs/FRGs for general momenta requires a truncation scheme. Such truncation schemes will be discussed starting with section IV. Many statements in the remainder of this section apply to the correct solution, and may be violated by any given truncation. E. g., any given truncation scheme will in general violate constraints, which are imposed by the symmetries of the theory. Furthermore, any truncation scheme will neglect part of the physics. The best which can be achieved by truncation is that for a given topic these vi

$$\begin{aligned} k \partial_k \text{ (loop diagram)}^{-1} &= - \text{ (loop diagram)} - \text{ (loop diagram)} \\ &+ \frac{1}{2} \text{ (loop diagram)} + \frac{1}{2} \text{ (loop diagram)} \\ &- \frac{1}{2} \text{ (loop diagram)} + \text{ (loop diagram)} \\ k \partial_k \text{ (loop diagram)}^{-1} &= \text{ (loop diagram)} + \text{ (loop diagram)} \\ &- \frac{1}{2} \text{ (loop diagram)} + \text{ (loop diagram)} \end{aligned}$$

FIG. 4: Functional RG equations for the gluon and ghost propagator. Filled circles denote dressed propagators and empty circles denote dressed vertex functions. Crosses denote insertions of the regulators.

olations are sub-leading effects. Depending on the question to be answered and the truncation the irrelevance of violations may be established a-priori or a-posteriori. This will be discussed further in the following sections.

In Landau gauge, there is another property of the DSE/FRG equations for general amputated Green's functions. The equations for fully transversal Green's functions  $\Gamma_{\text{transversal}}^{(m,n)}$  close on themselves,

$$\Gamma_{\text{transversal}}^{(m,n)} = \text{FRG/DSE}[\{\Gamma_{\text{transversal}}^{(m,n)}\}]. \quad (10)$$

This follows directly from the fact that all internal gluon legs are transversal due to the transversality of the gluon propagator in Landau gauge, and transversal projections on the external gluon legs leaves us with purely transversal vertices on the rhs of the DSE/FRG equations. It is this subset of equations, (10), which carries the full dynamics of the theory.

The DSE/FRG equations for Green's functions with at least one longitudinal gluon leg,  $\Gamma_{\text{longitudinal}}^{(m,n)}$ , depend both on the set of longitudinal as well as transversal Green's functions,

$$\Gamma_{\text{longitudinal}}^{(m,n)} = \text{FRG/DSE}[\{\Gamma_{\text{longitudinal}}^{(m,n)}\}, \{\Gamma_{\text{transversal}}^{(m,n)}\}], \quad (11)$$

and hence is not closed. The  $\Gamma_{\text{longitudinal}}^{(m,n)}$  also have to satisfy STIs, that in general imply non-trivial cancellations between different diagrams in the DSE/FRG equations in (11). This will be be discussed in detail in section III.

Here we discuss standard perturbation theory as a prime example for these non-trivial cancellations: In leading order perturbation theory, in which only the one-loop graphs on the right-hand side in Fig. 3 or the integrated flow of Fig. 4 contribute, none of the loops is transverse individually, and only their sum is, up to higher order in the coupling constant.

#### D. Analytical solutions and confinement

There are so far two limits in which an analytical determination of the leading contribution of Green's functions can be performed without referring to ad-hoc truncations.

One case is the far ultraviolet, where, due to asymptotic freedom, it is possible to determine the leading behavior of Green's functions with analytical means. This leading part can be determined with great accuracy, and including higher order corrections of the leading part. Asymptotic freedom also grants the luxury of proving that the leading part of the Green's functions, as determined by perturbation theory, is in fact uniquely the correct one.

The other kinematical limit is that of the far infrared, i.e. for external momentum scales  $p^2 \ll \Lambda_{\text{QCD}}^2$ . There, a general power law behavior of the dressing functions of one-particle irreducible Green's functions with  $2n$  external ghost legs and  $m$  external gluon legs has been derived [6, 63]:

$$\Gamma^{(n,m)}(p^2) \sim (p^2)^{(n-m)\kappa+(1-n)(d/2-2)}. \quad (12)$$

Here,  $d$  is the space-time dimension. Below we shall restrict ourselves to the most important case  $d = 4$ . Eq. (12) is the unique self-consistent 'scaling' solution of the full, untruncated tower of DSEs and FRGs [10].

An important consequence of (12) is the presence of a nontrivial infrared fixed point in the running couplings related to the primitively divergent vertex functions of Yang-Mills theory [6]:

$$\begin{aligned} \alpha^{gh-gl}(p^2) &= \frac{g^2}{4\pi} G^2(p^2) Z(p^2) \sim \frac{\text{const}_{gh-gl}}{N_c}, \\ \alpha^{3g}(p^2) &= \frac{g^2}{4\pi} [\Gamma^{0,3}(p^2)]^2 Z^3(p^2) \sim \frac{\text{const}_{3g}}{N_c}, \\ \alpha^{4g}(p^2) &= \frac{g^2}{4\pi} \Gamma^{0,4}(p^2) Z^2(p^2) \sim \frac{\text{const}_{4g}}{N_c}, \end{aligned} \quad (13)$$

for  $p^2 \rightarrow 0$ . Here  $G(p^2)$  is the dressing function of the ghost propagator and  $Z(p^2)$  the corresponding one for the gluon. The appearance of these infrared fixed points is independent of the precise value of  $\kappa$ , although the numerical values of the pre-factors are influenced indirectly [6].

In terms of gluon and ghost propagators

$$\begin{aligned} D_{\mu\nu}(p) &= \left( \delta_{\mu\nu} - \frac{p_\mu p_\nu}{p^2} \right) D(p^2) \\ &= \left( \delta_{\mu\nu} - \frac{p_\mu p_\nu}{p^2} \right) \frac{Z(p^2)}{p^2} \\ D_G(p) &= -\frac{G(p^2)}{p^2} \end{aligned} \quad (14)$$

the solutions (12) yield the power laws

$$Z(p^2) \sim (p^2)^{-\kappa_A}; \quad G(p^2) \sim (p^2)^{-\kappa_C} \quad (15)$$

with  $\kappa = \kappa_C = -\kappa_A/2$  in four dimensions. For this solution the anomalous dimension  $\kappa$  is known to be positive [3, 4],  $\kappa > 0$ , one therefore finds an infrared divergent ghost dressing function and an infrared vanishing gluon dressing function. For  $\kappa = 1/2$  the gluon propagator (14) is finite at zero momentum,  $0 < D(0) < \infty$ , whereas for  $\kappa > 1/2$  even the gluon propagator is vanishing in the infrared.

Note that the conservation of global color charge implies that  $\kappa_C > 0$  in the Kugo-Ojima confinement scenario [53]. This already enforces scaling [10] with the relation  $\kappa_A = -2\kappa_C$ . In fact the Gribov-Zwanziger scenario of confinement [35, 36, 57] even implies  $\kappa = \kappa_C = -\kappa_A/2 > 1/2$ . In addition, a confinement criterion for quarks was recently put forward that links the infrared behavior of ghost and gluon propagators to the order parameter of quark confinement, the Polyakov loop [33]. Here quark confinement results in the constraint  $\kappa > 1/4$  for the scaling solution [33]. Numerical and analytical infrared solutions for propagators obtained in truncation schemes [1, 4, 5, 29, 32, 64] satisfy the set of constraints by the Kugo-Ojima and the Gribov-Zwanziger scenario as well as the confinement criterion of [33].

The absence of scaling implies the decoupling of (some) degrees of freedom. A solution of this type has been discussed in [15, 16, 17, 18, 19, 20, 37, 38, 39, 40] and is given by:

$$Z(p^2) \sim p^2; \quad G(p^2) \sim \text{const.} \quad (16)$$

We refer to this type of solution as the 'decoupling solution'. It does not satisfy the set of constraints by the Kugo-Ojima and the Gribov-Zwanziger scenario, but satisfies the quark confinement criterion of [33]:  $3\kappa_A - 2\kappa_C < -2$ . Note that the latter criterion is independent of the scenario and comes from the demand of a vanishing order parameter for quark confinement. We also emphasize that the difference between the scaling solution (15) and the decoupling solution (16) is not the possible appearance of an infrared finite gluon propagator,  $\kappa_A = -1$ , but the presence or absence of the scaling relation  $\kappa_A = -2\kappa_C$ . We will come back to this point in detail in section IV, where we discuss numerical solutions of the Dyson-Schwinger equations for the ghost and gluon propagators.

### III. SLAVNOV-TAYLOR IDENTITIES AND RENORMALIZATION

#### A. Slavnov-Taylor identities

We now discuss the relevance of Slavnov-Taylor identities when it comes to identifying acceptable solutions from functional equations. We present general arguments why in transverse gauges these identities cannot serve to generate constraints on the transversal Green's functions of the theory. This is then demonstrated explicitly for

the case of the infrared behavior of the ghost dressing function.

Slavnov-Taylor identities (STI) relate various Green's functions. STIs are most conveniently represented in terms of the Zinn-Justin equation for the effective action, see e.g. [24, 26],

$$\int_x \left( \frac{\delta\Gamma}{\delta K_\mu^a} \frac{\delta\Gamma}{\delta A_\mu^a} + \frac{\delta\Gamma}{\delta L^a} \frac{\delta\Gamma}{\delta c^a} + \frac{\partial_\mu A_\mu^a}{\xi} \frac{\delta\Gamma}{\delta \bar{c}^a} \right) = \text{cut-off terms}, \quad (17)$$

together with translation invariance of the anti-ghost,

$$\int_x \left( \frac{\delta\Gamma}{\delta \bar{c}^a} - \partial_\mu \frac{\delta\Gamma}{\delta K_\mu^a} \right) = 0. \quad (18)$$

Here  $\xi$  denotes the parameter of linear covariant gauges, which has to be set to zero for Landau gauge. The cut-off terms on the right hand side of eq. (17) depend on the chosen renormalization scheme and are in particular present when a momentum cut-off is used, as necessary in all systematic numerical treatments. We come back to this point in subsection III B below. Within the FRG approach the rhs of (17) is given in a closed form as a one loop term similar to the flow equation (9), see [23, 24, 25, 26, 27]. In general the identities (17) and (18) are solved in a given truncation to the effective action  $\Gamma$  that lead to truncated FRG/DSE-systems for propagators and vertices.

In Landau gauge the constraints from the STIs decouple from the dynamics of the system, if no further assumptions are made [64, 65]. The reason is that the STIs relate the longitudinal parts, or more precisely the BRST-projected parts, of vertex functions and propagators to loops of the transversal gluon propagator, the ghost propagator and vertices, schematically written as

$$\Gamma_{\text{longitudinal}}^{(m,n)} = \text{STI}[\{\Gamma_{\text{longitudinal}}^{(m,n)}\}, \{\Gamma_{\text{transversal}}^{(m,n)}\}], \quad (19)$$

to be compared with the FRG/DSE-equations for the longitudinal Green's functions, (11). In turn the FRG/DSE-equations for the transversal propagator and vertices close on themselves, (10), as already argued in section II C. Formally, (11), (19) can be resolved for

$\Gamma_{\text{longitudinal}}^{(m,n)}[\Gamma_{\text{transversal}}^{(m,n)}]$ . In non-Abelian gauge theories the above hierarchy does not close, there is no self-contained subset of relations for a subset of longitudinal vertex functions  $\{\Gamma_{\text{longitudinal}}^{(m,n)}\}$ , whereas in Abelian theories this is indeed possible [65].

However, most truncations rely on an expansion in vertex functions and hence  $n, m \leq n_{\text{max}}, m_{\text{max}}$ . Then also the hierarchy of non-Abelian STIs might be closed. In such a case the STIs (19) can be resolved and provide integral constraints for the transversal Green's functions  $\Gamma_{\text{transversal}}^{(m,n)}$ .

We conclude that strictly speaking the STIs can only fix the longitudinal parts of 1PI correlation functions. If, however, the following further regularity assumption would be implemented,

$$|\partial_{p_i} \Gamma^{(m,n)}| < \infty, \quad (20)$$

transversal and longitudinal correlation functions are linked, and the STIs also directly constrain the transversal correlation functions, for a detailed discussion see [65]. Such assumptions have been widely used in Abelian theories, see e.g. [65, 66, 67]. In non-Abelian theories results obtained from (20) have to be discussed cautiously as (20) certainly fails already at the level of the propagators.

Having said this, we proceed by exploring the consequences of (17) for the correlation functions. Instead of using the functional identity (17) that allows for a systematic discussion of the truncation scheme involved, the STIs for correlation functions are sometimes also derived by BRST variations of vacuum expectation values of product of field operators.

Similar to functional equations, the STIs relate Green's functions with a different number of external legs. We would like to discuss this fact within a relevant example. The BRST variation of the expectation value of  $A_\mu^a A_\nu^b \bar{c}^c$  will produce a Slavnov-Taylor identity involving the ghost and gluon propagators, the three-gluon vertex and the ghost-gluon vertex, and the irreducible ghost-gluon scattering kernel. A simple way to obtain this identity is by using BRST invariance on the expectation value  $\langle A_\mu^a A_\nu^b \bar{c}^c \rangle$ , yielding

$$0 = -\langle A_\nu^b \bar{c}^c \partial_\mu c^a \rangle - \langle A_\mu^a \bar{c}^c \partial_\nu c^b \rangle + \frac{1}{\xi} \langle A_\mu^a A_\nu^b \partial_\rho A_\rho^c \rangle - g(f^{ade} \langle A_\mu^e A_\nu^b c^d \bar{c}^c \rangle + f^{bde} \langle A_\mu^a A_\nu^e c^d \bar{c}^c \rangle). \quad (21)$$

The last term can be dropped in lowest order perturbation theory due to the explicit factor  $g$ , but this is not possible in non-perturbative calculations.

Nonetheless, the standard truncation of the effective action used in the literature within numerical investigations of FRG- and DSE systems takes into account full

momentum-dependent propagators, and RG-improved ghost-gluon, three-gluon and four-gluon vertices. All higher vertices, in particular the ghost-gluon scattering kernel, are usually left out.

As the DSEs for the propagators depend on the bare and full ghost-gluon and three- and four gluon vertices,

but do not depend explicitly on the ghost-gluon scattering kernel  $\langle A^2 c\bar{c} \rangle$ , this is apparently a viable truncation. Moreover, the latter vertex has been also left out in most applications to vertex DSEs, which labels such a truncation as a minimally self-consistent DSE-approach in a vertex truncation.

However, the scattering kernel does appear in diagrams in the FRG equations for both the gluon and ghost propagators. This comes about as both hierarchies of equations represent different resummation schemes and using the same vertex truncation at the level of the effective action

implements different truncation schemes. Note that it is precisely this structure that allowed for the uniqueness proof of the IR-asymptotics from both sets of equations [10], and is also the key ingredient for the important consistency checks for the results of correlation functions.

Let us nonetheless proceed and neglect the four-point function appearing in (21). This has been done previously, either completely [1, 19, 20, 67] or only its connected part [68].

Following [67], as has been done in general [1, 19, 20], the STI takes the form

$$q_\nu \Gamma_{\mu\nu\rho}^{(0,3)}(p, q, k) = \frac{G(q^2)}{Z(p^2)} (\delta_{\mu\nu} p^2 - p_\mu p_\nu) \Gamma_{\nu\rho}(p, q; k) - \frac{G(q^2)}{Z(k^2)} (\delta_{\nu\rho} k^2 - k_\nu k_\rho) \Gamma_{\mu\nu}(k, q; p). \quad (22)$$

Herein  $\Gamma_{\mu\nu}$  is implicitly defined by the ghost-gluon vertex

$$\Gamma_\mu^{(2,1)}(p, q; k) = p_\nu \Gamma_{\nu\mu}(p, q; k)$$

where  $k$  is the gluon momentum. It is the ghost-gluon scattering kernel, but with two external legs contracted, and thus not the same quantity as appearing in (21), which is not contracted and has thus one momentum ar-

gument more. By virtue of Lorentz symmetry it can be expanded as [67]

$$\Gamma_{\nu\mu}(k, q; p) = \delta_{\mu\nu} a - q_\mu p_\nu b + p_\mu k_\nu c + p_\nu k_\mu d + k_\mu k_\nu e,$$

with five unknown functions  $a, \dots, e$ .

When contracting the left-hand side of (22) with  $p_\mu k_\rho$ , it vanishes [67]. From this the relation

$$\frac{G(q^2)}{Z(k^2)} a(p, q, k) - \frac{G(p^2)}{Z(k^2)} a(q, p, k) - pq \left( \frac{G(q^2)}{Z(k^2)} b(p, q, k) - \frac{G(p^2)}{Z(k^2)} b(q, p, k) \right) + pk \frac{G(q^2)}{Z(k^2)} d(p, q, k) - qk \frac{G(p^2)}{Z(k^2)} d(q, p, k) = 0, \quad (23)$$

and cyclic permutations thereof, have been obtained [67]. However, this condition is actually weaker than possible: By the assumption of a tree-level color structure, the three-gluon vertex has to be totally antisymmetric in any pair of momentum and Lorentz-indices. Hence, it is sufficient to contract (22) just with either  $p_\mu$  or  $k_\nu$  to make the left-hand side vanish. Since on the right-hand side always one term is transverse w.r.t. the momentum which has been used to contract it, it follows that, e. g. when contracting with  $k_\rho$  that

$$0 = \frac{G(q^2)}{Z(p^2)} (\delta_{\mu\nu} p^2 - p_\mu p_\nu) \Gamma_{\nu\rho}(p, q; k) k_\rho.$$

This leaves the condition (after relabeling)

$$a(p, q, k) - pq b(p, q, k) + pk d(p, q, k) = 0, \quad (24)$$

and cyclic permutations. This is a condition implying certain cancellations between the dressing functions of the ghost-gluon vertex, independent of the values of the dressing functions of the propagators. In particular, the

structure is very reminiscent of the one which will be obtained in section IV for the longitudinal part of the ghost-gluon vertex to ensure transversality of the gluon propagator in the far infrared.

Furthermore the equality (24) implies the relation (23), independent of the value of the propagator dressing functions. The dressing functions  $a, \dots, e$  in eq. (23) are an (arbitrary) splitting of the two independent dressing functions of the ghost-gluon vertex [67], and therefore can exhibit in principle any type of behavior in the infrared satisfying (24). However, as the non-longitudinal component of the ghost-gluon vertex is infrared finite, while the longitudinal one seems to be vanishing [7], the behavior of  $a, \dots, e$  is not necessarily regular (as assumed in [20]).

We conclude that these results do not provide any constraints on the ghost dressing function. Furthermore, the condition (24) has been derived from the approximation (22) to the complete STI (21) and hence cannot be used to exclude certain types of solutions for the Green's functions as has been attempted in [20].

## B. Renormalization

We now come back to the issue of renormalization-dependent terms in the STIs. The functional equations displayed in Figs. 3 and 4 and the corresponding STIs apply to the renormalized propagators and hence are equations for finite Green's functions. Whereas this finiteness trivially carries over to general truncation schemes for the functional RG equation due to the regulator insertion, it is not evident in general truncations of the DSE. The reason for the latter intricacy originates in the fact that the finiteness of the propagator DSEs is achieved by cancellations of divergencies stemming from different diagrams in Fig. 3. In gauge theories these cancellations are partially governed by Slavnov-Taylor identities. We conclude that finiteness of the DSEs requires a careful discussion of the renormalization procedure as well as the Slavnov-Taylor identities in the presence of a given regularization.

For any numerical implementation such a regularization involves a momentum cut-off. It is well-known that a momentum cut-off scheme might necessitate additive renormalization, in particular in gauge theories where a momentum cut-off deforms the Slavnov-Taylor identities. Indeed, within the flow equation approach the momentum cut-off is explicitly introduced at the level of the functional integral and the corresponding modified Slavnov-Taylor identities are explicitly known [24]. Furthermore it has been shown how to deduce a self-consistent renormalization scheme for DSEs with additive counter terms in the presence of a momentum cut-off from the corresponding FRG equations [24]. In particular the latter entail a gluonic mass term that tends towards zero if the momentum cut-off is removed. For the DSEs this translates into quadratic divergencies that have to be canceled identically by mass-type counter-terms [69]. This leads to a well-defined unique treatment of truncational divergencies in the DSEs that renders the equation finite within a given general truncation. In particular these considerations enable to interpret the longitudinal part of the gluon propagator DSE: It has to be fully canceled by the related longitudinal counter-term in order to restore transversality of the fully renormalized propagator. In turn this uniquely fixes the transversal part. Previously, this procedure has implicitly been applied within numerical applications to DSEs [5, 69, 70, 80].

Having said this we emphasize that multiplicative renormalization should still be possible for the DSEs within specific schemes. Indeed such a scheme is much wanted for as the modified Slavnov-Taylor identities for the DSEs in the presence of non-transversal counter terms are only implicitly known via the relations to the according flow equations. In a multiplicative scheme the standard Slavnov-Taylor identities can be used which completely decouple the longitudinal parts of the Green's functions from the DSEs of the transversal Green functions and render the latter system fully self-contained. Consequently such a choice optimizes the physics content of a given truncation. Moreover, for a multiplicative

scheme it is possible to renormalize the complete system with five renormalization constants in Landau gauge, the two wave-function renormalization constants of the ghost and the gluon,  $\tilde{Z}_3$  and  $Z_3$ , as well as the three primitively divergent vertices, the ghost-gluon vertex with  $\tilde{Z}_1$ , the three-gluon vertex with  $Z_1$ , and the four-gluon vertex with  $Z_4$ . The latter three can all be related to a single renormalization constant,  $Z_g$  of the coupling  $g_0$ .

## IV. GHOSTS AND GLUONS FROM DYSON-SCHWINGER EQUATIONS

In this section we report on explicit solutions for the Dyson-Schwinger equations of the ghost and gluon propagators. These equations involve three fully dressed vertices: the ghost-gluon, three-gluon and four-gluon vertices. For the purpose of the present work we shall restrict ourselves to the well-established method of constructing ansaetze for the vertices taking into account as much information from the vertex DSEs as possible. We would like to emphasize, however, that by now we have accumulated enough information on the details of these vertex equations [6, 7, 11, 12, 13, 44, 52, 83] such that a simultaneous treatment of the DSEs for propagators and vertices is within reach in the near future.

Here we investigate the possibility of two different types of solutions for the ghost and gluon propagators in the infrared. In the course of this study we need to carefully address technical issues like boundary conditions on the DSEs, transversality of the gluon propagator in Landau gauge and the appearance of quadratic divergencies in the gluon DSE once a hard momentum cutoff is introduced for the numerical treatment of the equations. To illustrate our points we use two different truncation schemes for the DSEs. The first one has been developed in Refs. [5, 70] and produced results in quantitative agreement with corresponding lattice calculations in the ultraviolet and low-momentum regions. Deviations in the mid-momentum regime around one GeV are of the order of 20 percent and well understood from the nature of the truncation scheme. Qualitative differences in the deep infrared are at the heart of our study here and will be addressed below. The second scheme will be constructed in the next subsections. It serves to study the influence of technical issues related to (the breaking of) gauge invariance on the possible types of solutions of the DSEs. In turn we will address a connection between renormalization and boundary conditions in the ghost DSE and the issues of quadratic divergencies and transversality in the gluon DSE.

### A. A boundary condition in the ghost DSE

The ghost DSE is given by

$$\frac{1}{G(p^2; \mu^2)} = \tilde{Z}_3 - \tilde{Z}_1 \frac{g^2(\mu^2) N_c}{(2\pi)^4} \int d^4 q \Gamma_\mu^{(2,1)(0)}(p, q; \mu) \left( \delta_{\mu\nu} - \frac{k_\mu k_\nu}{k^2} \right) \frac{Z(k^2; \mu^2) G(q^2; \mu^2)}{k^2 q^2} \Gamma_\nu^{(2,1)}(q, p; \mu) \quad (25)$$

with the bare ghost-gluon vertex  $\Gamma_\mu^{(2,1)(0)}$ , its dressed counterpart  $\Gamma_\mu^{(2,1)}$  and the momentum routing  $k = p + q$ . The ghost renormalization function  $\tilde{Z}_3$  and the ghost-gluon vertex renormalization function  $\tilde{Z}_1$  both depend on the renormalization point  $\mu^2$ .

The equation as it stands is multiplicatively renormalizable as recalled explicitly in appendix B. It then follows that the choice of  $g^2(\mu^2)$ , which implicitly fixes  $\mu^2$ , cannot have any impact on the type of solutions one finds in the DSEs. All multiplicatively renormalizable solutions must exist between infinitesimally small  $g^2$  (asymptotic freedom; large  $\mu^2$ ) and a potential maximum value that can be derived from the infrared behavior of the couplings (13). To discuss this further we rewrite the ghost DSE schematically as

$$\frac{1}{G(p^2; \mu^2)} = \tilde{Z}_3 - \tilde{Z}_1 g^2(\mu^2) I(p; \mu) \quad (26)$$

and subtract the equation at  $p^2 = 0$

$$\frac{1}{G(p^2; \mu^2)} = \frac{1}{G(0; \mu^2)} - \tilde{Z}_1 g^2(\mu^2) (I(p; \mu) - I(0; \mu)). \quad (27)$$

This way we got rid of the renormalization factor  $\tilde{Z}_3$  in exchange for the boundary condition  $G(0; \mu^2)$ . One can now explicitly choose between solutions of the scaling type (15) or the decoupling type (16) by varying  $G(0; \mu^2)$  [4, 20]. Clearly,  $G(0; \mu^2)^{-1} = 0$  corresponds to an infrared diverging ghost dressing function. This choice corresponds to the 'horizon condition' derived by Zwanziger to account for the presence of the Gribov-horizon when evaluating correlation functions [35, 36, 71]. The other option,  $G(0; \mu^2) = \text{const.}$ , produces an infrared finite ghost dressing function by construction. If the unsubtracted equation (26) is used these conditions translate into equivalent ones for the renormalization constant  $\tilde{Z}_3$ . From this it is clear that it is instructive but not necessary to subtract the ghost equation exactly at zero momentum. One can find both solutions for an arbitrary subtraction point  $s$ , if the boundary conditions on  $G(s; \mu^2)$  are selected appropriately. This is a consequence of renormalization group invariance. For the scaling solution the equivalence of boundary conditions for  $G(0; \mu^2)$  and  $G(s; \mu^2)$  has been explicitly demonstrated in [72].

In [20] the two types of solutions have been shown to coexist in a numerical treatment of the ghost DSE alone. Below we demonstrate that self-consistent solutions of both types exist when the ghost and gluon Dyson-Schwinger equations are solved simultaneously.

## B. The gluon DSE: quadratic divergencies

Having discussed the ghost DSE on general grounds we now focus on the gluon DSE. To this end we need to specify an explicit truncation scheme for the fully dressed vertices involved. As stated above, one such scheme has been constructed in refs. [5, 70]. We first shortly summarize this truncation before we qualitatively improve upon it.

In general, the dressed ghost-gluon vertex  $\Gamma_\mu^{(2,1)}$  can be written as

$$\Gamma_\mu^{(2,1)}(p, q; k) = i q_\mu A(q, k) + i k_\mu B(q, k) \quad (28)$$

where  $p$  and  $q$  are the incoming and outgoing ghost momenta respectively and  $k$  is the gluon momentum.  $A(q, k)$  and  $B(q, k)$  denote the two dressing functions of the vertex with  $A(q, k) \rightarrow 1$  and  $B(q, k) \rightarrow 0$  return the tree-level vertex. The dressing functions  $A(q, k)$  and  $B(q, k)$  have been subject to investigations in the continuum [4, 7] and  $A(q, k)$  also on the lattice [51, 52] and found to only mildly deviate from the tree-level behaviors. Furthermore it has been shown in [4] that the infrared behavior of the ghost-gluon system is only mildly affected by possible vertex dressings. This justifies the truncation

$$\Gamma_\mu^{(2,1)}(p, q; k) = i q_\mu, \quad (29)$$

i. e., the replacement of the fully dressed ghost-gluon vertex in the DSEs by its tree-level counterpart. This truncation has been used in [5, 70] and [20].

The situation is somewhat more complicated for the three-gluon vertex. Here an ansatz  $\Gamma_{\mu\nu\rho}^{(0,3)}(p, q) = \Gamma_{\mu\nu\rho}^{(0,3)(0)} \Gamma^{3g}(p, q)$  has been chosen in [5] with the tree-level vertex  $\Gamma_{\mu\nu\rho}^{(0,3)(0)}$  and dressing function  $\Gamma^{3g}(p, q)$  that leads to solutions for the ghost and gluon DSE with the correct one-loop running from resummed perturbation theory. The ansatz is given by eq. A1 in the appendix. Furthermore it has been shown in [70] that this choice of the vertex also leads to solutions which respect multiplicative renormalizability of the gluon DSE. Contributions involving the four-gluon interaction have been neglected in [5]. For the scaling solution this affects only the intermediate momentum regime, as shown there. For the decoupling solution the omission of the four-gluon vertex may also have an impact at low momenta. This needs to be explored in future work.

In general a truncation scheme such as the one summarized here faces the problem of quadratic divergencies appearing in the gluon DSE. These have been dealt with in the past by explicit subtraction procedures on the level of the integrands [5, 72, 80], numerical subtractions on

the level of the right hand side of the gluon DSE [69] or subtractions of purely quadratically divergent term involving only the perturbative form of the ghost and gluon dressing functions [17]. Although conceptually different all these procedures lead to similar results if correctly implemented.

Here we introduce yet another procedure which takes into account the general considerations of subsection III B. Recall that the introduction of a hard momentum cut-off into the theory modifies the Slavnov-Taylor identities. This modification has its biggest effects on

momentum scales near the cut-off. An improved truncation scheme that avoids the related problem of quadratic divergencies therefore should work with vertex modifications at these scales. Such a scheme is constructed in the following. We devise ansaetze for the ghost-gluon and the three-gluon vertices that resolve the issue of quadratic divergencies. The resulting ghost and gluon DSEs are then multiplicatively renormalizable in the first place without the need for additional subtraction procedures.

The procedure turns out to be straightforward. For the ghost-gluon vertex we start with the general ansatz

---


$$\Gamma_\mu^{(2,1)}(p, q, k) = iq_\mu \left( 1 + A + B \frac{p^2}{k^2} + C \frac{p^2}{q^2} + D \frac{q^2}{k^2} + E \frac{q^2}{p^2} + F \frac{k^2}{p^2} + G \frac{k^2}{q^2} + H \frac{(p \cdot q)^2}{p^2 q^2} + I \frac{(p \cdot k)^2}{p^2 k^2} + J \frac{(q \cdot k)^2}{q^2 k^2} \right), \quad (30)$$


---

which includes all possible modifications of the vertex in terms of dimensionless combinations up to powers of two in momenta and angles. Here  $p$  is the incoming ghost momentum,  $q$  is the one of the outgoing ghost and  $k = p - q$  is the momentum attached to the gluon leg. The coefficients  $A..J$  are assumed to be constant in momentum. One can then perform an ultraviolet analysis of the gluon DSE and the ghost DSE along the lines of ref. [5, 70] and restrict the possible values of the coefficients by demanding the following conditions:

- No quartic and quadratic divergencies should appear in the ghost loop of the gluon DSE and the ghost-gluon loop in the ghost DSE.
- The logarithmic divergencies of these loops should

remain the same as for the bare ghost-gluon vertex, i.e. as in perturbation theory.

This restricts the coefficients of (30) to a family of solutions which depend on the explicit values of two of the constants  $A..J$ . Setting as many of these constants to zero as possible one arrives at the surprisingly simple form

$$\bar{\Gamma}_\mu^{(2,1),UV}(p, q, k) = iq_\mu \left( 1 - \frac{q^2}{p^2} \right). \quad (31)$$

A similar procedure for the three-gluon vertex produces the result

---


$$\bar{\Gamma}_{\rho\nu\sigma}^{(0,3),UV}(q, p) = \Gamma_{\rho\nu\sigma}^{(0,3)(0)}(q, p) \Gamma^{3g}(p, q) \left( 1 - \frac{140}{51} - \frac{52}{17} \frac{p^2}{k^2} + \frac{89}{51} \frac{p^2}{q^2} + \frac{52}{17} \frac{q^2}{k^2} - \frac{26}{17} \frac{k^2}{q^2} + \frac{104}{17} \frac{(q \cdot k)^2}{q^2 k^2} \right), \quad (32)$$


---

where  $\Gamma_{\rho\nu\sigma}^{(0,3)(0)}(q, p)$  is the bare three-gluon vertex and  $\Gamma^{3g}(p, q)$ , given in appendix A, has been introduced in [5, 70] to reproduce the correct logarithmic running of the gluon in the ultraviolet. The additional, power-like vertex dressings in (31) and (32) serve to avoid quadratic divergencies in the ultraviolet momentum regime. As discussed above, the power-like modifications should affect the vertices only for momenta close to the ultraviolet regulator. We therefore multiply (31) and (32) with appropriate damping factors that cancel these terms smoothly with decreasing momenta. The explicit form of the damping factors will be given in the next subsection.

### C. Transversality

Next we come back to the issue of transversality, continuing the discussion from section III A. In Landau gauge, the gluon propagator is transverse and this property is reflected by the structure of the full, untruncated gluon DSE. For symmetry conserving regularization schemes this property can be maintained in truncation schemes that satisfy the Slavnov-Taylor identities. However, even truncation schemes satisfying a finite number of STIs are extremely hard to implement in numerical calculations. There one usually has to resort to

a momentum cut-off. As a consequence spurious longitudinal terms are generated in the gluon DSE that need to be projected out by contracting the gluon DSE with a transverse projector. This problem has been overlooked in [17]. There a truncation has been used that is formally transverse under dimensional regularisation while it is not when a hard cutoff is used in the numerical calculations. Consequently, in contradiction to their claims, the numerical solutions presented in [17] are not strictly transversal.

In general, projection onto the transverse part of the right hand side of the gluon DSE, as done in [5] guarantees reliable results. Nevertheless it is interesting to construct a truncation scheme that in addition minimizes the spurious longitudinal terms. This is the purpose of this subsection.

As is apparent from the analysis of ref. [5] transversality is naturally maintained in the ultraviolet where perturbation theory is at work. In the infrared, however, the situation is different and sizeable longitudinal components of the gluon are present. To improve this situation we consider the most general form for the dressed ghost-gluon vertex, eq. (28), and contract the ghost-loop in the gluon DSE with a longitudinal projector, thereby projecting onto the spurious terms. Apart from trivial factors one obtains the combination

$$q_\mu \frac{p_\mu p_\nu}{p^2} \Gamma_\nu^{(2,1)}(p, q; k) = q_\mu \frac{p_\mu p_\nu}{p^2} (k_\nu A(k, p) + p_\nu B(k, p)) \stackrel{!}{=} 0 \quad (33)$$

where  $p$  is the gluon momentum and  $q$  and  $k = q - p$  are the two ghost momenta. This is reminiscent of

equation (24). From this relation we find the condition  $B(k, p) = -A(k, p) \frac{k \cdot p}{p^2}$  which eliminates the spurious terms and makes the ghost-loop transverse. As will be shown later this construction is sufficient to render the gluon DSE transversal on the level of numerical accuracy. Note, however, that a more general construction for  $B$  is possible such that exact transversality of the gluon DSE for all momenta is guaranteed.

As a result the dressed ghost-gluon vertex in the infrared can be written as

$$\bar{\Gamma}_\mu^{(2,1),IR}(p, q; k) = iq_\mu A(q, k) - ik_\mu \frac{k \cdot q}{k^2} A(q, k) \quad (34)$$

in the momentum labeling of eq. (28) where  $k$  is the gluon momentum. It is important to note that the additional term in eq. (34) is longitudinal in the gluon momentum, i.e. it does not contribute to the ghost-loop in Landau gauge but merely serves to eliminate non-transverse artefacts. Thus the infrared analysis of the ghost loop performed in [4] and the value of  $\kappa$  remain unchanged.

Longitudinal contributions to the ghost-gluon vertex have been calculated from the vertex-DSE in [7] and found to vanish for large momenta, in agreement with perturbation theory. We therefore need to multiply the longitudinal structure in (34) by appropriate damping factors to account for this behavior. Furthermore we choose  $A(q, k) = 1$  as in the truncation scheme of the previous section.

Taking into account the ultraviolet modifications (31) and (32) of the previous subsection we then find our final ansaetze for the ghost-gluon and three-gluon vertices

$$\bar{\Gamma}_\mu^{(2,1)}(p, q; k) = iq_\mu \left( 1 - \frac{q^2}{p^2} f_{UV}(p, q; k) \right) - ik_\mu \left( \frac{k \cdot q}{k^2} f_{IR}(p, q; k) \right) \quad (35)$$

$$\bar{\Gamma}_{\rho\nu\sigma}^{(0,3)}(q, p) = \Gamma_{\rho\nu\sigma}^{(0,3)(0)}(q, p) \Gamma^{3g}(q, p) \left( 1 - \left[ \frac{140}{51} - \frac{52}{17} \frac{p^2}{k^2} + \frac{89}{51} \frac{p^2}{q^2} + \frac{52}{17} \frac{q^2}{k^2} - \frac{26}{17} \frac{k^2}{q^2} + \frac{104}{17} \frac{(q \cdot k)^2}{q^2 k^2} \right] f_{UV}(p, q; k) \right) \quad (36)$$

with appropriate damping factors

$$f_{UV}(p, q; k) = \left( \frac{p^2 q^2 k^2}{(p^2 + \Lambda_{UV}^2)(q^2 + \Lambda_{UV}^2)(k^2 + \Lambda_{UV}^2)} \right)^2; \quad f_{IR}(p, q; k) = \frac{\Lambda_{IR}^6}{(p^2 + \Lambda_{IR}^2)(q^2 + \Lambda_{IR}^2)(k^2 + \Lambda_{IR}^2)}, \quad (37)$$

for the infrared and ultraviolet modifications of the vertices. The dressing  $\Gamma^{3g}(p, q)$  is given in appendix A. The

resulting forms of the equations for the ghost and gluon DSEs are given by

$$\begin{aligned} \frac{1}{Z(p^2)} &= Z_3 + g^2 \frac{N_c}{3} \int \frac{d^4 q}{(2\pi)^4} \frac{\bar{M}(p^2, q^2, (p-q)^2)}{p^2 q^2} G(q^2) G((p-q)^2) \\ &\quad + g^2 \frac{N_c}{3} \int \frac{d^4 q}{(2\pi)^4} \frac{\bar{Q}(p^2, q^2, (p-q)^2)}{p^2 q^2} Z(q^2) Z((p-q)^2) \Gamma^{3g}(q, p) , \end{aligned} \quad (38)$$

$$\frac{1}{G(p^2)} = \tilde{Z}_3 - g^2 N_c \int \frac{d^4 q}{(2\pi)^4} \frac{\bar{K}(p^2, q^2, (p-q)^2)}{p^2 q^2} G(q^2) Z((p-q)^2) . \quad (39)$$

These forms are similar to the ones of the previously used truncation scheme of [5, 70]. The effect of the vertex modifications (35) and (36) is hidden in the kernels  $\bar{K}, \bar{M}, \bar{Q}$  which are given in appendix A together with the original kernels  $K, M, Q$  of ref. [5].

The two free scale parameters  $\Lambda_{IR}$  and  $\Lambda_{UV}$  are fixed by the following procedure: Once a numerical solution of the DSEs has been obtained we project the right hand side of the gluon DSE onto the longitudinal component of the gluon propagator. This component is then minimized by changing the two scales. We find that this procedure is insensitive to  $\Lambda_{UV}$  in a window of roughly  $\Lambda/2 < \Lambda_{UV} < \Lambda$ , where  $\Lambda$  is the ultraviolet cutoff in our numerical procedure. In practice we choose the lower bound of this interval. The infrared modification of the ghost-gluon vertex is important in the regime where the infrared asymptotics sets in. Consequently we find an optimized value of  $\Lambda_{IR} \approx 300$  MeV. This choice leads to spurious longitudinal components of the gluon propagator in the mid-momentum regime of the order of less than one permille, i.e. of the order of the numerical error of our calculations. In the infrared and ultraviolet momentum regime these terms are even smaller by orders of magnitude.

Finally we wish to point out that the technical improvements of this section are also extremely useful when it comes to calculations at finite temperature, where quadratic divergencies represent a much more severe problem than at zero temperatures. Improvements along the lines suggested here have been anticipated in [72].

#### D. Renormalization conditions

Having specified the truncation scheme it remains to detail the renormalization conditions imposed on our system of equations. To discuss these we need to recall the definition of the running coupling from the ghost-gluon vertex [1]

$$\alpha(p^2) = \alpha(\mu^2) \frac{G(p^2; \mu^2)^2 Z(p^2; \mu^2)}{G(\mu^2; \mu^2)^2 Z(\mu^2; \mu^2)} \quad (40)$$

where the dependence of the dressing functions on the renormalization point  $\mu^2$  is given explicitly. Note that the right hand side of the equations is independent of  $\mu^2$ , i.e., it is a renormalization group invariant. This defi-

nition follows straightforwardly from the Slavnov-Taylor identity

$$\tilde{Z}_1 = Z_g Z_3 \tilde{Z}_2^2 \quad (41)$$

where the renormalization function  $\tilde{Z}_1$  of the ghost-gluon vertex is always finite in Landau gauge. For a bare ghost-gluon vertex, as chosen here,  $\tilde{Z}_1 = 1$ . Then, in the momentum subtraction scheme ( $\overline{MOM}$ ) defined in [1] the renormalization condition  $G(\mu^2; \mu^2)^2 Z(\mu^2; \mu^2) = 1$  is imposed, which we also adopt here. Then  $G(\mu^2; \mu^2)$  and  $Z(\mu^2; \mu^2)$  are not independent of each other. In practice one chooses a value for  $\alpha(\mu^2)$ , which in turn determines the renormalization point  $\mu^2$ . In [20] the special choice  $G(\mu^2; \mu^2) = Z(\mu^2; \mu^2) = 1$  has been used, which in general leads to  $\tilde{Z}_1 = \text{const} \neq 1$  by virtue of the STI (41).

The definition (13) of the running coupling represents a mass independent renormalization scheme. This, however, may not be adequate for the decoupling solution with  $0 < D(0) < \infty$ . In this case one should separate the 'massive' part of the gluon propagator from the part proportional to  $p^2$ . Therefore we introduce

$$D^{-1}(p^2) = \frac{p^2}{Z(p^2)} = \frac{1}{\bar{Z}(p^2)} (p^2 + m^2) , \quad (42)$$

with the renormalization group invariant mass parameter  $m$ . Note that this splitting is not unique and one obtains an additional free normalization parameter  $\bar{Z}(0)$ . The running of  $\bar{Z}$  then enters the running coupling by

$$\alpha(p^2) = \alpha(\mu^2) \frac{G(p^2; \mu^2)^2 \bar{Z}(p^2; \mu^2)}{G(\mu^2; \mu^2)^2 \bar{Z}(\mu^2; \mu^2)} \quad (43)$$

and the renormalization condition is given by  $G(\mu^2; \mu^2)^2 \bar{Z}(\mu^2; \mu^2) = 1$ . Independently of this renormalization condition one has the freedom to vary  $\bar{Z}(0)$ , which together with the boundary condition  $G(0)$  determines the value of the infrared fixed point of this coupling. This is further discussed in the next subsection.

For all our numerical results except the ones presented in the appendix B, where we show the independence on this choice, we have used  $\alpha(\mu^2) = 1$ .

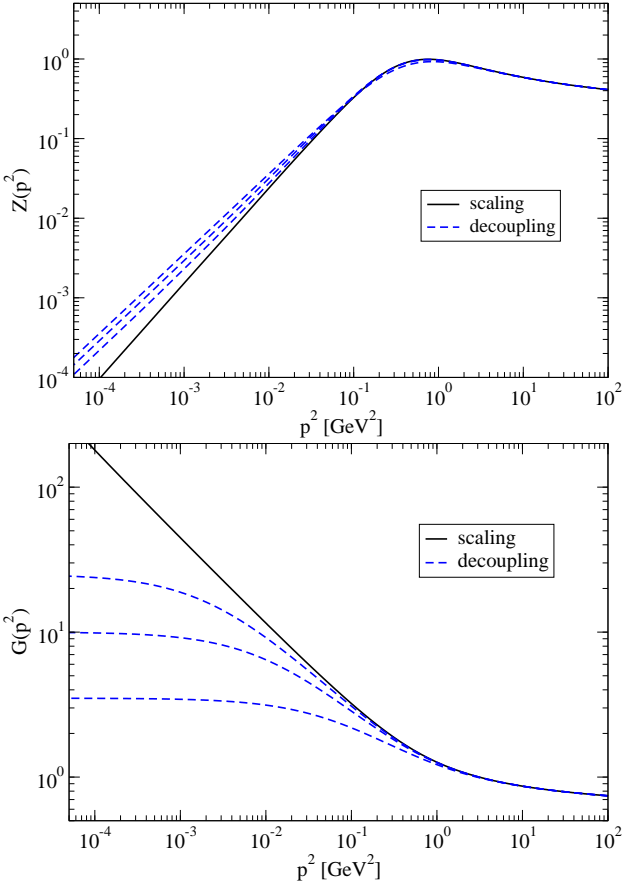


FIG. 5: Numerical solutions for the ghost and gluon dressing function with different boundary conditions  $G(0)$ . The (artificial) longitudinal components of the gluon propagator are not displayed, since they are of the order of less than one permille, i.e. of the order of the numerical error of our calculations. All results shown here are obtained from our novel truncation scheme. Differences to the scheme defined in [5, 70] are, however, only very small and would not be visible in the plots.

### E. Numerical results

Our numerical solutions for the ghost and gluon dressing functions are shown in Fig. 5. The corresponding momentum scale has been fixed by best-possible matching of the gluon dressing function to the corresponding one on the lattice, cf.

### V. SEC:LATTICE

. Thus we inherit the lattice scale. All results displayed are obtained from our novel truncation scheme. Differences to the scheme defined in [5, 70] are, however, only very small and would not be visible in the plots. This provides additional justification that the old scheme already represented a reliable result. Transversality is manifest in our new truncation scheme; the longitudinal components

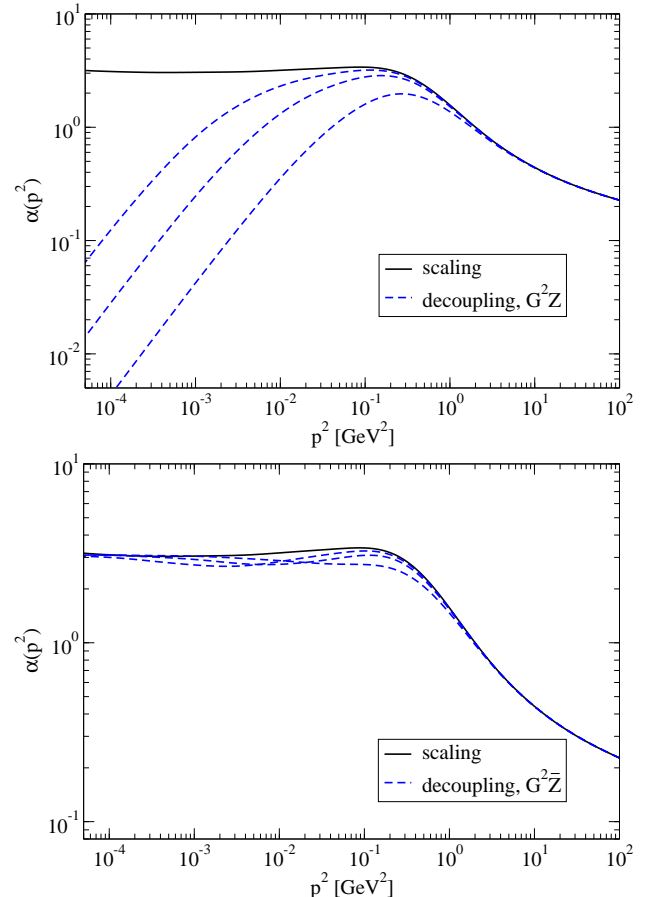


FIG. 6: The running coupling for the two types of solutions, defined as  $\alpha(p^2) = \alpha(\mu^2)G(p^2)^2Z(p^2)$  (top diagram) and  $\alpha(p^2) = \alpha(\mu^2)G(p^2)^2\bar{Z}(p^2)$  (bottom diagram).

of the propagator (not shown in the figure) are smaller than one permille and therefore of the same size as the numerical error of our calculation. Quadratic divergencies do not appear and the numerical solutions respect multiplicative renormalizability, see appendix B.

By varying the boundary condition  $G(0, \mu^2)$  we are able to generate both, a solution of the scaling type I, eq. (15)), with  $G^{-1}(0, \mu^2) = 0$  and a continuous set of decoupling solutions characterized by a finite value  $G(0, \mu^2)$ . Shown are results for three different values of  $G(0, \mu^2)$ . The corresponding gluon propagator is either massive in the sense that  $D(0) = \lim_{p^2 \rightarrow 0} Z(p^2)/p^2 = \text{const.}$  for decoupling, or has the power like behavior (15) with  $\kappa = \kappa_C = (93 - \sqrt{1201})/98 \approx 0.595353$  [4] in the case of scaling. In the ultraviolet momentum region, both types of solutions are almost identical, as expected. The running couplings are shown in Fig. 6. For the scaling solution one observes the infrared fixed point known from previous studies, whereas the coupling for the decoupling solution falls with  $p^2$  in the infrared when the mass-independent definition (40) is used (top diagram of Fig. 6). If, however, we employ the mass-dependent definition (43) (bottom diagram of Fig. 6) the resulting

coupling develops a fixed point in the infrared. The value of this fixed point is an additional free parameter and has been fixed at  $\alpha(0) \approx 3$ , i.e. at approximately the value of the fixed point of the scaling solution. Note that these couplings still show variations with changes of  $G(0)$  at intermediate momenta from  $0.1 - 1$  GeV.

In the light of these findings we wish to make the following comments:

- In principle one has to face the problem that an inadequate ultraviolet renormalization may result in an infrared mass for the gluon reflecting the breaking of BRST-invariance by the momentum cutoff. We explicitly checked that this is not the case for both our scaling and the decoupling solution; the solutions are independent of the cutoff  $\Lambda$  imposed in the loop integrals. In particular this is true for  $D(0)$ .
- We also assessed the behavior of the dressing functions under a change of the renormalization point  $\mu^2 \rightarrow \nu^2$ , i.e. we chose  $\alpha(\nu^2) = 0.5$  and  $G(\nu^2; \nu^2)^2 Z(\nu^2; \nu^2) = 1$ . Again, by varying  $G(0, \nu^2)$  we find both types of solutions and the resulting ghost and gluon dressing functions are related to the ones at  $\alpha(\mu^2) = 1$  by renormalization factors, as they should. The explicit results can be found in appendix B. We therefore conclude that there is no notion of a 'critical' coupling distinguishing the two types of solutions as claimed in [20]. Instead it is solely the boundary condition  $G(0, \mu^2)$  that matters.
- We wish to point out that the decoupling solution with an infrared finite gluon propagator necessarily entails an infrared finite ghost dressing function (up to logarithms) as long as the ghost-gluon vertex does not contain any nontrivial power-laws [10, 20]. This situation is also realized in [17], where henceforth  $\kappa_C = 0$  must be realized. This is compatible with part of the fits they deduce from their numerical solutions.
- The issue of transversality is separate from the question of which types of solutions are realized in a particular truncation scheme. In non-transverse truncation schemes longitudinal components of the gluon propagator only constitute a problem if they are back-fed into the equation by the use of a non-transverse projection method of the gluon DSE. This has carefully been avoided in the truncation scheme of [5] which consequently delivered very similar results as the new scheme employed in this section.
- We wish to emphasize again that either (i) global BRST symmetry is unbroken, then the decoupling solution would imply the breaking of global color symmetry as indicative for a Higgs phase of the theory. Or, (ii), in a confining phase the decoupling

solution implies the breaking of global BRST symmetry and therefore does not agree with the Kugo-Ojima confinement scenario. Indeed, all known BRST-quantizations indicating towards an infrared finite ghost even break off-shell BRST [38, 40]. Therefore it is not clear how to construct a physical state space in the decoupling case. In terms of Green's functions this implies that it is not known how to construct physical observables in general. In our opinion this is a serious problem. In addition the decoupling solution is in contradiction with the Gribov-Zwanziger confinement scenario due to its finite ghost dressing function [75]. All in all, the status of the decoupling solutions is therefore clearly different from the scaling solution, which agrees with both, the Kugo-Ojima and the Gribov-Zwanziger scenarios.

It is furthermore interesting to compare our results to corresponding ones from DSEs on a torus. In [5, 76] solutions from the ghost and gluon DSE on a torus have been discussed which did not connect to a scaling type of solution even if very large volumes were taken. In a later work [77] the renormalization conditions for the torus solutions have been reconsidered and adapted such that the scaling solution in the infinite volume/continuum limit has been reproduced. The status of the solutions found in [5, 76], however, remained somewhat unclear. From the results of this work we are now in a position to clarify this issue. The different renormalization conditions on the torus employed in [5, 76] and [77] are in one-to-one correspondence to the boundary condition  $G^{-1}(0, \mu^2)$  for the continuum DSEs investigated in this work. The infinite volume/continuum limit of the solutions found in [5, 76] is therefore given by one of the decoupling type of solutions reported in this work.

Finally we wish to point out that the parameter  $G^{-1}(0, \mu^2)$  corresponds to a related one in the Zwanziger-Lagrangian approach [78] to infrared Yang-Mills theory. There, a mass parameter can be introduced which produces decoupling solutions for non-vanishing mass [40] and scaling solutions for vanishing mass, see e.g. [79] and refs. therein. The latter is in agreement with the original Gribov-Zwanziger scenario.

## VI. GHOSTS AND GLUONS FROM THE FUNCTIONAL RENORMALIZATION GROUP

The DSE-analysis of the previous sections can be repeated within the functional RG. In order to facilitate the access to the FRG-literature on Landau gauge Yang-Mills, e.g. [23, 24, 25, 26, 27, 28, 29, 30, 31, 32, 33], we present the results in standard FRG-notation and provide the dictionary to the DSE-computations. The results shown here are preliminary results taken from [64]. We shall be brief on the details of this analysis and only discuss the relation between the renormalization procedure in the DSE of section IV and that in the FRG.

Furthermore we comment on the truncation and discuss its relation to that used in the DSE. The renormalization conditions are contained in appropriately chosen initial conditions for the effective action  $\Gamma_\Lambda$  at the ultraviolet scale  $\Lambda$ . Indeed it has been shown in [24] that the integrated flow equations define a set of DSEs within a consistent BPHZ-type renormalization scheme. This system reads for the effective action

$$\Gamma = \Gamma_\Lambda + \frac{1}{2} \text{Tr} \ln \Gamma^{(2)} - \frac{1}{2} \int_\Lambda^0 \frac{dk'}{k'} \text{Tr} \dot{\Gamma}_{k'}^{(2)} \frac{1}{\Gamma_{k'}^{(2)} + R_{k'}}. \quad (44)$$

The first term on the rhs of (44) comprises the renormalization conditions as an initial condition as can be seen via the comparison of the second field derivatives of (44) and (38). The second term on the rhs of (44) contains one loop contributions to Green's functions  $\Gamma^{(2n,m)}$  with full propagators and vertices, the third integral term contains RG-improvement terms such as the two-loop diagrams in the DSEs. In the present truncation we need the (inverse) propagators  $\Gamma_A^{(2)} = \Gamma^{(0,2)}$ ,  $\Gamma_C^{(2)} = \Gamma^{(2,0)}$ ,

$$\begin{aligned} \Gamma_{\mu\nu}^{(2)ab}(p^2) &= Z_A(p^2)p^2\delta^{ab}\left(\delta_{\mu\nu} - \frac{p_\mu p_\nu}{p^2}\right) + \text{longitud.}, \\ \Gamma_C^{(2)ab}(p^2) &= Z_C(p^2)p^2\delta^{ab}, \end{aligned} \quad (45)$$

as well as the vertices  $\Gamma^{(2,1)}, \Gamma^{(0,3)}, \Gamma^{(0,4)}$ . For the vertices we refer to the parameterization in section IV and to [24, 29, 64]. The wave function renormalization functions  $Z_A, Z_C$  relate to the dressing functions  $Z(p^2), G(p^2)$  as

$$Z_A(p^2) = \frac{1}{Z(p^2)}, \quad Z_C(p^2) = \frac{1}{G(p^2)}, \quad (46)$$

whereas  $Z_3, \tilde{Z}_3$  and  $\tilde{Z}_1$  are defined with  $\Gamma_\Lambda^{(2,0)}, \Gamma_\Lambda^{(0,2)}$  and  $\Gamma_\Lambda^{(2,1)}$ . Note that RG-invariance of the FRG-equation is automatically guaranteed by the separate RG-invariance of each term in (44), and hence the invariance of the FRG solution under a change of the renormalization scale  $\mu$ . The scaling and decoupling solutions (at  $k = 0$ ) are now adjusted via fine-tuning of  $\tilde{Z}_3$  as in the DSEs. Indeed, the ghost FRG can be mapped into the corresponding DSE and one can directly use eq. (27). Finally, the truncation is optimized [24, 34] by an appropriate choice of the regulator function  $R$ . The optimized regulator employed for the present work has been derived from functional optimization in [24]. It has been already shown for the present truncation in [29] that optimized regulators lead to the same analytic expressions for  $\kappa$ 's and  $\alpha(0)$  in the scaling solution as for the DSE equations,  $\kappa_C \approx 0.595353, \alpha(0) \approx 3$ . Other regulators lead to scaling solutions with slightly varying  $\kappa$ ,  $\kappa \in [.539\dots, .59535\dots]$ , for a specific choice see also [32]. Note that the above interval serves as an estimate on the systematic error of the present FRG and also DSE truncation. Furthermore it has been argued in [30] that the lower value relates to finite volume studies, providing a

link to the torus DSE analyses in [5, 76, 77]. More details on the present FRG analysis will be presented in [64].

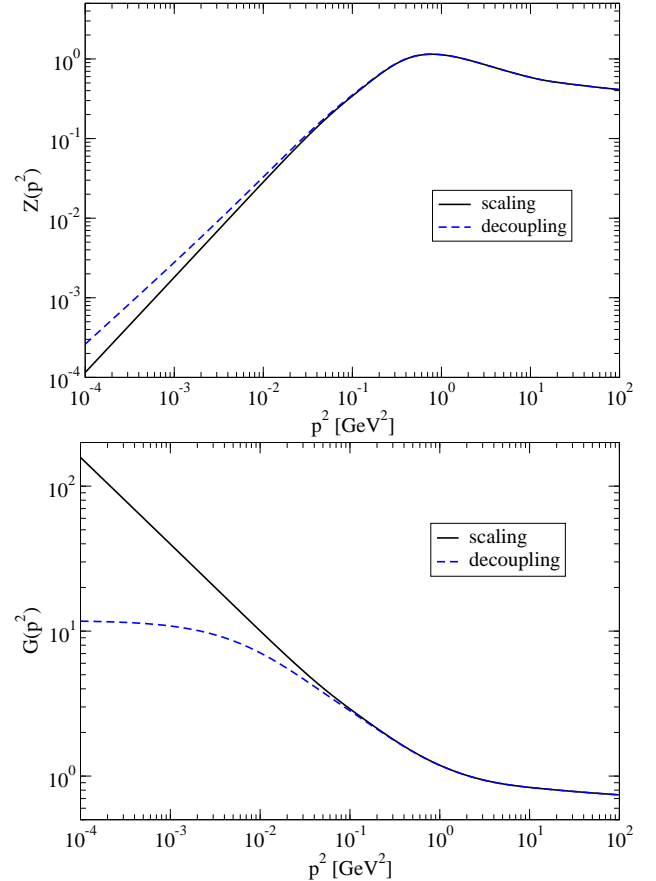


FIG. 7: Numerical solutions for the ghost and gluon dressing function with two different boundary conditions  $G(0)$  calculated from the FRGs.

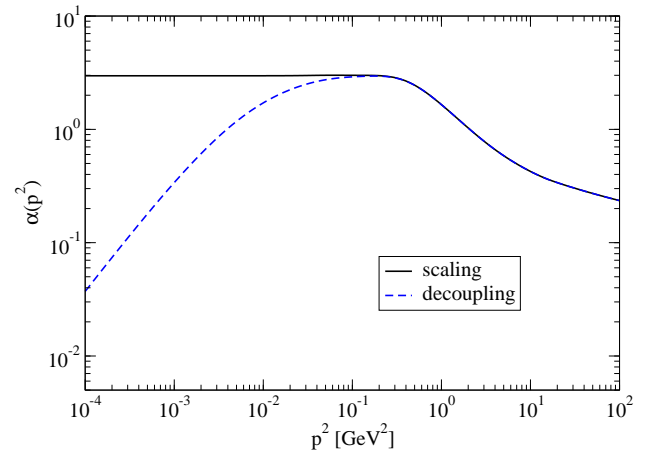


FIG. 8: The running coupling from the FRGs, defined as  $\alpha(p^2) = \alpha(\mu^2)G(p^2)^2Z(p^2)$ .

The numerical solutions from the FRGs are presented in Figs. 7 and 8. We show the scaling solution and

one representative for a decoupling solution. They agree qualitatively and to a large extent also quantitatively with the ones from the DSEs presented in the previous section. Therefore both frameworks support the conclusions discussed there. Quantitative differences in the mid-momentum regime can be attributed to the different diagrammatics used in both approaches. In summary we have discussed the equivalence and consistency of the renormalization procedure for both, DSEs and FRGs. Moreover, the FRG provides a consistent momentum cut-off regularization of the corresponding DSE equation via (44) and thus allows to deduce the modified STIs for the DSE in the presence of an ultraviolet momentum cut-off, see [24, 64]. A crucial difference in the present truncation is the tadpole diagram in the gluon FRG-equation that depends on the full four-gluon vertex. This incorporates two-loop contributions of the sunset diagram in the gluon DSE, see Fig. 3.

## VII. COMPARISON WITH LATTICE RESULTS

In the previous two sections we obtained two different types of solutions for the ghost and gluon propagators in the DSE and FRG approaches. It is certainly instructive to compare these results to the ones from lattice calculations. As became apparent from a number of works in the past years such a comparison is not unambiguous. Ideally one strives for a situation where exactly the same quantities are calculated in the continuum and on the lattice. However, this is currently not the case for a number of reasons. First, lattice calculations are necessarily done in a finite volume. It is therefore mandatory to take into account finite volume effects and zero mode contributions absent in the infinite volume/continuum limit. Second, one encounters finite size contributions due to the non-vanishing lattice spacing. Third, artefacts due to the gauge fixing procedure are different from the ones in a continuum formulation.

Before we discuss these issues further let us compare the continuum solutions with the lattice results of refs. [44, 81] in minimal Landau gauge. In the top diagram of fig. 9 we display the gluon dressing function from different approaches. At large momenta, where perturbation theory sets in, all results are in excellent agreement with each other. The DSE results as well as the FRG results in the intermediate regime show only a mild dependence of the type of solution, i.e. scaling or decoupling does not really matter here, as expected. As compared to the standard DSE results the dressing function from the functional RG approach is closer to the lattice data. From the discussion of the last section this was to be expected, since the FRG truncation included effects from the gluonic two-loop diagrams neglected in the DSE-truncation. Note that such contributions can be either included directly or phenomenologically by modifying the three-gluon interaction in the one-loop diagram also into the DSE framework, see e.g. [82].

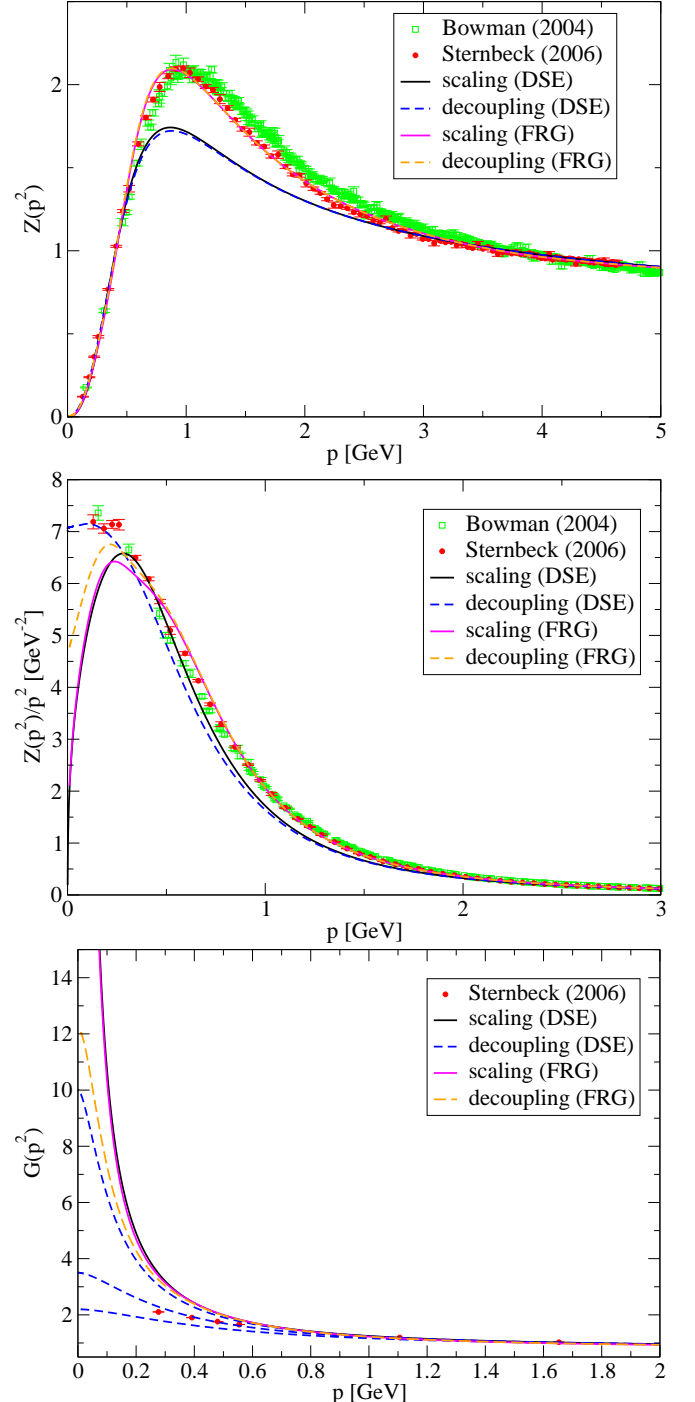


FIG. 9: Both type of solutions of sections IV and VI compared to lattice results in minimal Landau gauge from [44, 81].

The infrared behavior of the propagator functions for the gluon,  $D(p^2) = Z(p^2)/p^2$ , of both solutions are compared in the second panel of fig. 9. Clearly, the scaling solution comprises an infrared vanishing propagator, whereas the decoupling solutions are infrared finite. Changing the boundary condition  $G^{-1}(0, \mu^2)$  from zero to finite values first leads to a finite but small value for

$D(0)$  with the corresponding gluon propagator still being non-monotonous. From a certain minimal value of  $G^{-1}(0, \mu^2)$  on, this behavior changes and the gluon becomes a monotonously decreasing function of momentum. Such a monotonous behavior is also seen in the lattice data, which therefore clearly represent a decoupling type of solution for the gluon.

The third diagram of fig. 9 compares results for the ghost dressing function from the continuum approaches with the lattice data. Again we find that the lattice results resemble a decoupling type of solution, i.e. it seems from the plot that the corresponding value  $G(0, \mu^2)$  on the lattice would be finite.

In conclusion, the lattice results support a decoupling solution with broken BRST symmetry. The origin of this BRST breaking is currently not understood. It may be induced by one or more of the three aforementioned effects.

Finite volume corrections are unambiguously present and are sizeable even for large volumes [77]. However, recent calculations on very large lattices [46, 47, 49] have demonstrated that these corrections alone do not change the solution from a decoupling one to a scaling one. These results have been obtained on rather coarse lattices in the minimal Landau gauge<sup>1</sup>. Correcting for both effects has a significant impact.

Recently, it has been shown [54] that the gluon propagator, and in particular its value at zero momentum  $D(0)$ , are affected by discretization artifacts which originate from different possibilities to define the gauge field on the lattice. The consequences of such discretization artifacts are not yet studied in detail, but evidence has been found that is in favor of a scaling solution on very fine, large lattices [54].

Finally, the question of adequate gauge-fixing is of relevance. As discussed in the beginning the basic scenario is established in the absolute Landau gauge, and therefore the lattice calculations should be done in this gauge. However, the numerical implementation of this gauge is expensive, and hence most calculations so far have been done in the minimal Landau gauge. Nonetheless, it is known that at least the ghost propagator differs in both gauges, but the extent and volume-dependence is not known sufficiently well in four dimensions [48, 84]. Again, recently [56] evidence has been found which suggest that the absolute Landau gauge produces the scaling solution. However, only in three and two dimensions support for this has been found yet and only indications are so far available in four dimensions [48, 55, 56], mainly due to the computing time required in four dimensions. Extrapolations in the number of dimensions  $d$  make it nonetheless likely that also in four dimensions in the absolute

Landau gauge the propagators are scaling.

Hence both effects are in favor of a scaling solution. Nonetheless, the interplay of these effects and finite volume effects has not yet been fully investigated, and the situation in lattice gauge theory is not yet unambiguously resolved.

By comparison of the lattice and the functional results it seems furthermore tempting to conjecture that the scaling solution is in fact obtained in absolute Landau gauge, and the absolute Landau gauge is implemented in functional calculations by the implementation of the boundary condition  $G(0, \mu^2)^{-1} = 0$ . The good agreement of the massive solution to the lattice results in minimal Landau gauge, see Fig. 9, suggest further that the other boundary condition  $G(0, \mu^2)^{-1} \neq 0 < \infty$  seems to implement the minimal Landau gauge. However, final justification of this idea requires a clarification of the role of discretization artifacts [54] and other subtleties in defining the minimal Landau gauge [56].

Alternatively, one could check which solution satisfies the condition for absolute Landau gauge. One is the positivity of the ghost dressing function, which is given in both cases. The other is the requirement of minimizing the trace of the gluon propagator, equivalent to the condition (4) [56],

$$\mathcal{F}(D) = c \int p Z(p) dp, \quad (47)$$

with a positive constant  $c$  [56]. As is visible from Fig. 5 and 9, at low momenta the scaling solution is smaller for both the DSE and FRG results. At mid-momentum, both solutions are similar from the FRG, while from the DSEs the massive solution is somewhat smaller. This already shows that the question whether (47) is minimal for scaling or decoupling depends on the details of the truncation and therefore cannot be answered from the results plotted in Fig. 5 and 9.

Finally, we would like to mention two general issues. First, we expect that the general structure of the interplay between gauge fixing and the infrared behavior of Green's functions is general and also present in other gauges. Clear indications for such a picture are given in [85] for the case of Coulomb gauge. Second, we wish to emphasize that our discussion is independent of the number of colors,  $N_c$ , and therefore valid for  $SU(N_c)$ -Yang-Mills theory. In the DSE/FRG framework an indirect and very mild dependence of the ghost and gluon dressing functions on  $N_c$  is induced by sub-leading components of the four-gluon vertex [12], which only have an impact in the mid-momentum region. This mild dependence is also found in lattice calculations comparing the dressing functions for the cases of  $SU(2)$  and  $SU(3)$  [86, 87].

In fact, based on the structure of the DSEs it has been conjectured [88] that the scenario presented here can be extended to any (semi-)simple Lie-group without any qualitative change. First support for this conjecture

---

<sup>1</sup> Note that minimal Landau gauge may have ambiguities, that possibly lead to differing propagators or at least differing finite volume effects [56], in contrast to the unique definition of the absolute Landau gauge.

in the case of the exceptional Lie-group  $G_2$  in lattice calculations has been presented in [89].

### VIII. GLUON CONFINEMENT

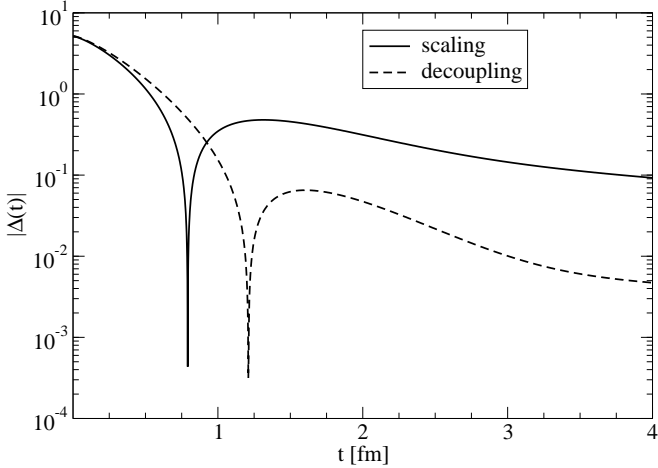


FIG. 10: The absolute value of the Schwinger function  $\Delta(t)$  plotted against time for both, the decoupling and scaling type of solutions. (The latter result with a slightly different scale has previously been published in [90].)

Finally we wish to investigate the issue of positivity violations in our two types of solutions. The confinement of gluons by the absence of a spectral representation of its propagator has been addressed e.g. in [1, 71, 90] with violation of positivity being a sufficient criterion for the absence of gluons from the physical part of the state space of QCD. For the scaling type of solutions with an infrared vanishing gluon propagator these violations can be shown analytically [71]. This is not so for the decoupling type of solutions. Thus to investigate this question one has to determine the Schwinger function

$$\Delta(t) = \int d^3x \int \frac{d^4p}{(2\pi)^4} \exp(ip \cdot x) D(p^2), \quad (48)$$

numerically. Here  $D(p^2) = Z(p^2)/p^2$  is the gluon propagator function. Our results for both type of solutions are shown in Fig. 10. Apart from some variations in the scale this type of behavior can be seen for all our decoupling solutions, i.e. it is independent of the value of  $G(0)$ . This statement, however, may depend on the truncation scheme.

From Fig. 10 it is plainly visible that, despite the differences in momentum space, the Schwinger function for both solutions is very similar. In particular, in both cases positivity is violated, and gluons are confined. This occurs for both cases at about the same scale of 1 fm, typical for the size of bound states.

Furthermore, both results for the Schwinger function are in qualitative agreement with corresponding results

from lattice calculations [91, 92]. Hence, despite the completely different status with respect to the Kugo-Ojima framework, both solutions do not describe propagating gluons.

In particular, the gluon is *not* characterized by a pole mass and an exponential decrease of a (positive) Schwinger function at large times. This implies that the mass parameter defined in (42) is also not a pole mass in the ordinary sense but at best a screening mass. In addition, a gauge-independent mass in a sense defined in [93] cannot be constructed. Hence, irrespective of its infrared properties, the gluon is never an ordinary massive particle.

### IX. SUMMARY AND DISCUSSION

We close with summarizing again some of our main results and conclusions. More detailed discussions have been provided in the related chapters.

We have obtained, in various truncations of DSEs and FRGs, a one-parameter family of solutions for the ghost and gluon dressing functions of Landau gauge Yang-Mills theory. We argued that Slavnov-Taylor identities cannot be used to discriminate between these, contrary to what has been claimed in [20]. In particular, transversality is not indicative in this respect. Our numerical solutions for both, scaling and decoupling, are transverse on the level of numerical accuracy. However, global symmetries are indicative: exactly one member of this family, the only one exhibiting scaling behavior, is consistent with the existence of a globally well-defined BRST charge. The remaining solutions are of a decoupling type and are not BRST-symmetric.

The appearance of the above mentioned one-parameter family of solutions in the DSEs and FRGs can be achieved by implementing boundary conditions [4, 20]. The scaling solution is in accordance with the Kugo-Ojima and Gribov-Zwanziger confinement scenarios and solely generated by the gauge fixing sector of the theory. In case of the decoupling solution the infrared dynamics is qualitatively different. We have argued that the latter type of dynamics cannot be color-confining and preserving BRST symmetry at the same time. Both solutions, however, satisfy the quark confinement criterion put forward in [33].

Finally, we would like to emphasize once more that neither solution corresponds to an ordinary massive gluon with a pole mass. Instead, in both cases the Schwinger function shows the presence of positivity violation and thus the gluon is not a free particle.

In conclusion, each member of the one-parameter family of solutions is confining.

#### Acknowledgments

We thank Reinhard Alkofer, Jens Braun, Joannis Papavassiliou, Olivier Pene, Kai Schwenzer and Lorenz von Smekal for useful discussions. A. M. was supported

by the FWF under grant number P20330, C. F by the Helmholtz-University Young Investigator Grant number VH-NG-332 and J. M. P. by the ExtreMe Matter Institute (EMMI).

## APPENDIX A: EXPLICIT EXPRESSIONS FOR THE DRESSING OF THE THREE-GLUON VERTEX AND THE INTEGRAL KERNELS

The ansatz for the three-gluon vertex used in our truncation includes the dressing function [5]

$$\Gamma^{3g}(p, q) = \frac{1}{Z_1} \frac{[G(y + \Lambda_{dec}^2) G(z + \Lambda_{dec}^2)]^{(1-a/\delta-2a)}}{[Z(y + \Lambda_{dec}^2) Z(z + \Lambda_{dec}^2)]^{(1+a)}} \quad (\text{A1})$$

with  $y = q^2$ ,  $z = (p - q)^2$ , the anomalous dimension  $\delta = -9/44$  of the ghost dressing function and the renor-

malization constant  $Z_1$  for the three-gluon vertex. The value of  $a$  is a free parameter which regulates the interaction strength of the vertex. In [5]  $a = 3\delta$  has been chosen. The scale  $\Lambda_{dec} \approx 500$  MeV is irrelevant for the scaling type of solutions since the gluon-loop including the three-gluon vertex becomes sub-leading at such small scales compared to the ghost loop. For decoupling type of solutions this scale implements decoupling within the three-gluon vertex. All results in this paper are qualitatively independent of  $\Lambda_{dec}$ . Quantitative changes in the decoupling solutions are at the percent level when varying this scale within reasonable bounds.

The kernels  $\bar{K}$ ,  $\bar{M}$  and  $\bar{Q}$  for the integral equations (38) and (39) are given by

$$\begin{aligned} \bar{M}(p^2, q^2, (p - q)^2) &= M(p^2, q^2, (p - q)^2) \\ &+ \left( (p - q)^2 \left[ -\frac{1}{2q^2} - \frac{1}{2p^2} \right] + \frac{(p - q)^4}{4p^2q^2} - \frac{1}{2} + \frac{p^2}{4q^2} + \frac{q^2}{4p^2} \right) f_{UV}(p^2, q^2; k^2), \end{aligned} \quad (\text{A2})$$

$$\begin{aligned} \bar{Q}(p^2, q^2, (p - q)^2) &= Q(p^2, q^2, (p - q)^2) \\ &+ \left( \frac{1}{(p - q)^4} \left[ \frac{39q^8}{68p^4} + \frac{236q^6}{51p^2} - \frac{1021q^4}{102} + \frac{66p^2q^2}{17} + \frac{181p^4}{204} + \frac{2p^6}{51q^2} \right] \right. \\ &+ \frac{1}{(p - q)^2} \left[ \frac{65q^6}{17p^4} - \frac{9923q^4}{408p^2} - \frac{365q^2}{51} + \frac{35p^2}{204} - \frac{30p^4}{17q^2} - \frac{67p^6}{408q^4} \right] \\ &+ (p - q)^2 \left[ \frac{5347}{204p^2} + \frac{674}{51q^2} + \frac{338q^2}{17p^4} + \frac{305p^2}{68q^4} \right] \\ &+ (p - q)^4 \left[ -\frac{689}{51p^2q^2} - \frac{485}{102q^4} - \frac{611}{68p^4} \right] + (p - q)^6 \left[ +\frac{557}{408p^2q^4} + \frac{13}{17p^4q^2} \right] + (p - q)^8 \frac{13}{68p^4q^4} \\ &\left. + \frac{250}{17} + \frac{287q^2}{51p^2} - \frac{2p^2}{51q^2} - \frac{229p^4}{204q^4} - \frac{65q^4}{4p^4} \right) f_{UV}(p^2, q^2; k^2) \end{aligned} \quad (\text{A3})$$

$$\begin{aligned} \bar{K}(p^2, q^2, (p - q)^2) &= K(p^2, q^2, (p - q)^2) \\ &+ \left( \frac{1}{(p - q)^4} \left[ \frac{p^2q^2}{4} - \frac{p^4}{2} + \frac{p^6}{4q^2} \right] - \frac{1}{(p - q)^2} \left[ \frac{p^2}{2} + \frac{p^4}{2q^2} \right] + \frac{p^2}{4q^2} \right) f_{UV}(p^2, q^2; k^2), \end{aligned} \quad (\text{A4})$$

with the original kernels  $K$ ,  $M$  and  $Q$  of the truncation

scheme of ref. [5, 70]:

$$\begin{aligned}
K(p^2, q^2, (p-q)^2) &= \frac{1}{(p-q)^4} \left( -\frac{(p^2-q^2)^2}{4} \right) + \frac{1}{(p-q)^2} \left( \frac{p^2+q^2}{2} \right) - \frac{1}{4}, \\
M(p^2, q^2, (p-q)^2) &= \frac{1}{(p-q)^2} \left( \frac{-1}{4} p^2 + \frac{q^2}{2} - \frac{1}{4} \frac{q^4}{p^2} \right) + \frac{1}{2} + \frac{1}{2} \frac{q^2}{p^2} - \frac{1}{4} \frac{(p-q)^2}{p^2}, \\
Q(p^2, q^2, (p-q)^2) &= \frac{1}{(p-q)^4} \left( \frac{1}{8} \frac{p^6}{q^2} + p^4 - \frac{18}{8} p^2 q^2 + q^4 + \frac{1}{8} \frac{q^6}{p^2} \right) \\
&\quad + \frac{1}{(p-q)^2} \left( \frac{p^4}{q^2} - 4p^2 - 4q^2 + \frac{q^4}{p^2} \right) \\
&\quad - \left( \frac{9}{4} \frac{p^2}{q^2} + 4 + \frac{9}{4} \frac{q^2}{p^2} \right) + (p-q)^2 \left( \frac{1}{p^2} + \frac{1}{q^2} \right) + (p-q)^4 \frac{1}{8p^2q^2}. \tag{A5}
\end{aligned}$$

---

## APPENDIX B: MULTIPLICATIVE RENORMALIZABILITY OF THE GHOST DSE

Multiplicative renormalizability of the ghost and gluon dressing functions implies the relations

$$\begin{aligned}
G(p^2, \mu^2) \tilde{Z}_3(\mu^2, \Lambda^2) &= G^0(p^2, \Lambda^2) \\
Z(p^2, \mu^2) Z_3(\mu^2, \Lambda^2) &= Z^0(p^2, \Lambda^2) \\
g(\mu^2) Z_g(\mu^2, \Lambda^2) &= g^0(\Lambda^2) \\
\Gamma_\mu^{(2,1)}(p, q, \mu^2) \tilde{Z}_1^{-1}(\mu^2, \Lambda^2) &= \Gamma_\mu^{(2,1)0}(p, q, \Lambda^2) \tag{B1}
\end{aligned}$$

between the bare dressing functions depending on a UV-cutoff  $\Lambda$  and denoted with superscript zero and the renormalized dressing functions depending on the renormalization point  $\mu^2$ .

Note that the right hand sides of eqs. (B1) are independent of the renormalization point. Thus a finite renormalization, i. e., a change in the renormalization point

from  $\mu^2$  to  $\nu^2$  is described by

$$\begin{aligned}
G(p^2, \nu^2) &= G(p^2, \mu^2) \frac{\tilde{Z}_3(\mu^2, \Lambda^2)}{\tilde{Z}_3(\nu^2, \Lambda^2)} \\
Z(p^2, \nu^2) &= Z(p^2, \mu^2) \frac{Z_3(\mu^2, \Lambda^2)}{Z_3(\nu^2, \Lambda^2)} \\
g(\nu^2) &= g(\mu^2) \frac{Z_g(\mu^2, \Lambda^2)}{Z_g(\nu^2, \Lambda^2)} \\
\Gamma_\mu^{(2,1)}(p, q, \nu^2) &= \Gamma_\mu^{(2,1)}(p, q, \mu^2) \frac{\tilde{Z}_1(\nu^2, \Lambda^2)}{\tilde{Z}_1(\mu^2, \Lambda^2)}. \tag{B2}
\end{aligned}$$

Furthermore we need the identity

$$\tilde{Z}_1 = Z_g Z_3^{1/2} \tilde{Z}_3. \tag{B3}$$

Now let us consider the Dyson-Schwinger equation for the ghost propagator

---


$$\frac{1}{G(p^2, \mu^2)} = \tilde{Z}_3(\mu^2, \Lambda^2) - \tilde{Z}_1(\mu^2, \Lambda^2) g^2(\mu^2) \int^\Lambda \frac{d^4 q}{(2\pi)^4} \frac{G(q^2, \mu^2)}{q^2} \frac{Z(k^2, \mu^2)}{k^2} \gamma_\mu P_{\mu\nu}^T(k) \Gamma_\nu^{(2,1)}(p, q, \mu^2) \tag{B4}$$

where  $P_{\mu\nu}^T(k) = \left( \delta_{\mu\nu} - \frac{k_\mu k_\nu}{k^2} \right)$  denotes the transverse projector and  $k_\mu = q_\mu - p_\mu$ . This equation is invari-

---

ant under a change of the renormalization point, since we have

$$\frac{1}{G(p^2, \nu^2)} = \frac{1}{G(p^2, \mu^2)} \frac{\tilde{Z}_3(\nu^2, \Lambda^2)}{\tilde{Z}_3(\mu^2, \Lambda^2)} \quad (B5)$$

$$= \tilde{Z}_3(\nu^2, \Lambda^2) - \frac{\tilde{Z}_3(\nu^2, \Lambda^2)}{\tilde{Z}_3(\mu^2, \Lambda^2)} \tilde{Z}_1(\mu^2, \Lambda^2) \frac{g^2(\nu^2) Z_g^2(\nu^2, \Lambda^2)}{Z_g^2(\mu^2, \Lambda^2)} \int^{\Lambda} \frac{d^4 q}{(2\pi)^4} \frac{G(q^2, \nu^2) \tilde{Z}_3(\nu^2, \Lambda^2)}{q^2 \tilde{Z}_3(\mu^2, \Lambda^2)} \frac{Z(k^2, \nu^2) Z_3(\nu^2, \Lambda^2)}{k^2 Z_3(\mu^2, \Lambda^2)} \gamma_\mu P_{\mu\nu}^T(k) \Gamma_\nu^{(2,1)}(p, q, \nu^2) \frac{\tilde{Z}_1(\mu^2, \Lambda^2)}{\tilde{Z}_1(\nu^2, \Lambda^2)} \quad (B6)$$

$$= \tilde{Z}_3(\nu^2, \Lambda^2) - \tilde{Z}_1(\nu^2, \Lambda^2) g^2(\nu^2) \int^{\Lambda} \frac{d^4 q}{(2\pi)^4} \frac{G(q^2, \nu^2)}{q^2} \frac{Z(k^2, \nu^2)}{k^2} \gamma_\mu P_{\mu\nu}^T(k) \Gamma_\nu^{(2,1)}(p, q, \nu^2) \frac{\tilde{Z}_1^2(\mu^2, \Lambda^2) Z_g^2(\nu^2, \Lambda^2) \tilde{Z}_3^2(\nu^2, \Lambda^2) Z_3(\nu^2, \Lambda^2)}{\tilde{Z}_1^2(\nu^2, \Lambda^2) Z_g^2(\mu^2, \Lambda^2) \tilde{Z}_3^2(\mu^2, \Lambda^2) Z_3(\mu^2, \Lambda^2)} \quad (B7)$$

$$= \tilde{Z}_3(\nu^2, \Lambda^2) - \tilde{Z}_1(\nu^2, \Lambda^2) g^2(\nu^2) \int^{\Lambda} \frac{d^4 q}{(2\pi)^4} \gamma_\mu \frac{G(q^2, \nu^2)}{q^2} \frac{Z(k^2, \mu^2)}{k^2} P_{\mu\nu}^T(k) \Gamma_\nu^{(2,1)}(p, q, \nu^2) \quad (B8)$$

This demonstrates explicitly that a solution  $G(p^2, \mu^2)$  of eq. (B4) and a solution  $G(p^2, \nu^2)$  of eq. (B8) are uniquely related by a multiplicative factor  $\frac{\tilde{Z}_3(\mu^2, \Lambda^2)}{\tilde{Z}_3(\nu^2, \Lambda^2)}$ . Thus a change of  $g^2$ , corresponding to  $g(\mu^2) \rightarrow g(\nu^2)$  with  $\mu^2 \neq \nu^2$  must not generate a qualitatively different solution.

Since our truncation respects multiplicative renormal-

izability this requirement is certainly respected. This is explicitly demonstrated in Fig. 11, where we compare our results for  $\alpha(\mu^2) = 1$  and  $\alpha(\mu^2) = 0.5$ . The resulting running coupling is clearly an RG-invariant, whereas the ghost and gluon dressing functions are related by finite re-normalization factors according to eq. (B2), as they should.

---

[1] L. von Smekal, A. Hauck and R. Alkofer, Annals Phys. **267** (1998) 1 [Erratum-ibid. **269** (1998) 182] [arXiv:hep-ph/9707327]; L. von Smekal, R. Alkofer and A. Hauck, Phys. Rev. Lett. **79** (1997) 3591 [arXiv:hep-ph/9705242].

[2] R. Alkofer and L. von Smekal, Phys. Rept. **353** (2001) 281 [arXiv:hep-ph/0007355].

[3] P. Watson and R. Alkofer, PRL **86** (2001) 5239 [hep-ph/0102332].

[4] C. Lerche and L. von Smekal, Phys. Rev. D **65**, 125006 (2002) [arXiv:hep-ph/0202194].

[5] C. S. Fischer and R. Alkofer, Phys. Lett. B **536** (2002) 177 [arXiv:hep-ph/0202202]; C. S. Fischer, R. Alkofer and H. Reinhardt, Phys. Rev. D **65** (2002) 094008 [arXiv:hep-ph/0202195].

[6] R. Alkofer, C. S. Fischer and F. J. Llanes-Estrada, Phys. Lett. B **611**, 279 (2005) [arXiv:hep-th/0412330].

[7] W. Schleifenbaum, A. Maas, J. Wambach and R. Alkofer, Phys. Rev. D **72**, 014017 (2005) [arXiv:hep-ph/0411052].

[8] C. S. Fischer, J. Phys. G **32**, R253 (2006) [arXiv:hep-ph/0605173].

[9] W. Schleifenbaum, M. Leder and H. Reinhardt, Phys. Rev. D **73** (2006) 125019 [arXiv:hep-th/0605115].

[10] C. S. Fischer and J. M. Pawłowski, Phys. Rev. D **75**, 025012 (2007) [arXiv:hep-th/0609009]; Phys. Rev. D in press, arXiv:0903.2193 [hep-th].

[11] R. Alkofer, M. Q. Huber and K. Schwenzer, arXiv:0801.2762 [hep-th]; arXiv:0904.1873 [hep-th].

[12] C. Kellermann and C. S. Fischer, Phys. Rev. D **78**, 025015 (2008) [arXiv:0801.2697 [hep-ph]].

[13] R. Alkofer, M. Q. Huber and K. Schwenzer, arXiv:0812.4045 [hep-ph].

[14] J. M. Cornwall, Phys. Rev. D **26** (1982) 1453.

[15] A. C. Aguilar and J. Papavassiliou, arXiv:0712.0780 [hep-ph].

[16] D. Binosi and J. Papavassiliou, Phys. Rev. D **77** (2008) 061702 [arXiv:0712.2707 [hep-ph]].

[17] A. C. Aguilar, D. Binosi and J. Papavassiliou, Phys. Rev. D **78**, 025010 (2008) [arXiv:0802.1870 [hep-ph]].

[18] Ph. Boucaud, Th. Bruntjen, J. P. Leroy, A. Le Yaouanc, A. Y. Lohkov, J. Micheli, O. Pene and J. Rodriguez-Quintero, JHEP **0606**, 001 (2006) [arXiv:hep-ph/0604056].

[19] Ph. Boucaud, J. P. Leroy, A. L. Yaouanc, J. Micheli, O. Pene and J. Rodriguez-Quintero, JHEP **0806**, 012 (2008) [arXiv:0801.2721 [hep-ph]].

[20] Ph. Boucaud, J. P. Leroy, A. Le Yaouanc, J. Micheli, O. Pene and J. Rodriguez-Quintero, JHEP **0806**, 099 (2008) [arXiv:0803.2161 [hep-ph]].

[21] J. C. R. Bloch, Phys. Rev. D **66** (2002) 034032 [arXiv:hep-ph/0202073].

[22] C. Wetterich, Phys. Lett. B **301** (1993) 90.

[23] D. F. Litim and J. M. Pawłowski, in *The Exact Renormalization Group*, Eds. Krasnitz et al, World Sci (1999)

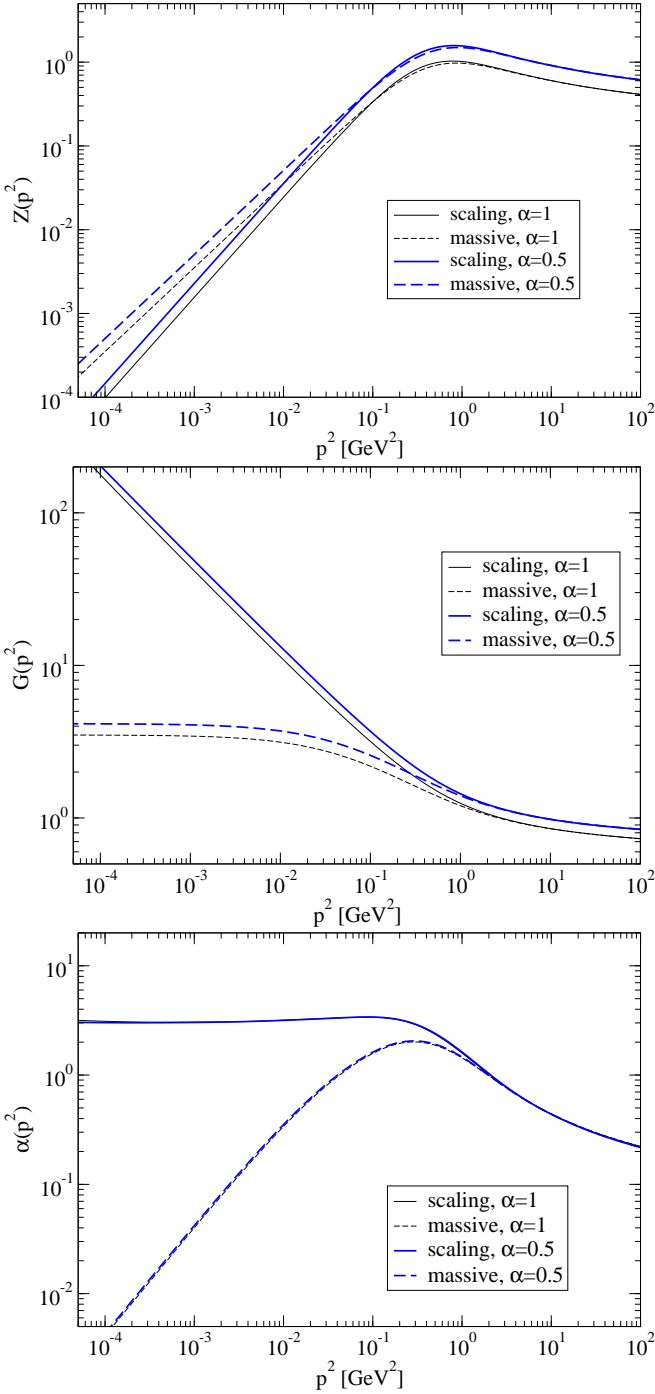


FIG. 11: Numerical results for the ghost and gluon dressing function as well as the running coupling for two different renormalization points.

168. [hep-th/9901063].

[24] J. M. Pawłowski, Annals Phys. **322** (2007) 2831. [arXiv:hep-th/0512261].

[25] H. Gies, arXiv:hep-ph/0611146.

[26] U. Ellwanger, Phys. Lett. B **335** (1994) 364 [arXiv:hep-th/9402077].

[27] M. Bonini, M. D'Attanasio and G. Marchesini, Nucl. Phys. B **437** (1995) 163 [arXiv:hep-th/9410138].

[28] U. Ellwanger, M. Hirsch and A. Weber, Z. Phys. C **69** (1996) 687 [arXiv:hep-th/9506019]; Eur. Phys. J. C **1** (1998) 563 [arXiv:hep-ph/9606468]; U. Ellwanger, Z. Phys. C **76** (1997) 721 [arXiv:hep-ph/9702309]; B. Bergnerhoff and C. Wetterich, Phys. Rev. D **57** (1998) 1591 [arXiv:hep-ph/9708425].

[29] J. M. Pawłowski, D. F. Litim, S. Nedelko and L. von Smekal, Phys. Rev. Lett. **93** (2004) 152002 [arXiv:hep-th/0312324].

[30] J. M. Pawłowski, D. F. Litim, S. Nedelko and L. von Smekal, AIP Conf. Proc. **756** (2005) 278 [arXiv:hep-th/0412326].

[31] J. Kato, arXiv:hep-th/0401068.

[32] C. S. Fischer and H. Gies, JHEP **0410** (2004) 048 [arXiv:hep-ph/0408089].

[33] J. Braun, H. Gies and J. M. Pawłowski, arXiv:0708.2413 [hep-th].

[34] D. F. Litim, Phys. Lett. B **486** (2000) 92 [arXiv:hep-th/0005245]. Phys. Rev. D **64** (2001) 105007 [hep-th/0103195]. Int. J. Mod. Phys. A **16** (2001) 2081 [arXiv:hep-th/0104221].

[35] D. Zwanziger, Phys. Rev. D **69**, 016002 (2004) [arXiv: hep-ph/0303028].

[36] D. Zwanziger, Phys. Rev. D **65**, 094039 (2002) [arXiv: hep-th/0109224]; Phys. Rev. D **67**, 105001 (2003) [arXiv: hep-th/0206053].

[37] D. Dudal, R. F. Sobreiro, S. P. Sorella and H. Verschelde, Phys. Rev. D **72**, 014016 (2005) [arXiv:hep-th/0502183].

[38] D. Dudal, S. P. Sorella, N. Vandersickel and H. Verschelde, arXiv:0711.4496 [hep-th].

[39] M. A. L. Capri, D. Dudal, V. E. R. Lemes, R. F. Sobreiro, S. P. Sorella, R. Thibes and H. Verschelde, Eur. Phys. J. C **52**, 459 (2007) [arXiv:0705.3591 [hep-th]].

[40] D. Dudal, J. A. Gracey, S. P. Sorella, N. Vandersickel and H. Verschelde, arXiv:0806.4348 [hep-th].

[41] O. Oliveira and P. J. Silva, arXiv:0705.0964 [hep-lat]; arXiv:0809.0258 [hep-lat].

[42] J. C. R. Bloch, A. Cucchieri, K. Langfeld and T. Mendes, Nucl. Phys. B **687**, 76 (2004) [arXiv:hep-lat/0312036].

[43] A. Sternbeck, E. M. Ilgenfritz, M. Müller-Preussker and A. Schiller, Phys. Rev. D **72**, 014507 (2005) [arXiv: hep-lat/0506007].

[44] A. Sternbeck, E. M. Ilgenfritz, M. Müller-Preussker, A. Schiller and I. L. Bogolubsky, PoS **LAT2006**, 076 (2006) [arXiv:hep-lat/0610053].

[45] A. Cucchieri and T. Mendes, Braz. J. Phys. **37**, 484 (2007) [arXiv:hep-ph/0605224].

[46] I. L. Bogolubsky, E. M. Ilgenfritz, M. Müller-Preussker and A. Sternbeck, PoS (LATTICE-2007) 290, arXiv: 0710.1968 [hep-lat]; A. Cucchieri and T. Mendes, PoS (LATTICE 2007) 297, arXiv:0710.0412 [hep-lat]; A. Sternbeck, L. von Smekal, D. B. Leinweber and A. G. Williams, PoS (LATTICE 2007) 340, arXiv:0710.1982 [hep-lat].

[47] A. Cucchieri and T. Mendes, Phys. Rev. Lett. **100**, 241601 (2008) [arXiv:0712.3517 [hep-lat]].

[48] I. L. Bogolubsky, G. Burgio, M. Müller-Preussker and V. K. Mitrjushkin, Phys. Rev. D **74**, 034503 (2006) [arXiv:hep-lat/0511056]; I. L. Bogolubsky *et al.*, Phys. Rev. D **77**, 014504 (2008) [Erratum-ibid. D **77**, 039902 (2008)] [arXiv:0707.3611 [hep-lat]].

[49] A. Cucchieri and T. Mendes, arXiv:0804.2371 [hep-lat].

[50] C. Parrinello, Phys. Rev. D **50** (1994) 4247, [arXiv:hep-lat/9405024]; P. Boucaud, J. P. Leroy,

J. Micheli, O. Pene and C. Roiesnel, JHEP **9810**, 017 (1998), [arXiv:hep-ph/9810322].

[51] E. M. Ilgenfritz, M. Muller-Preussker, A. Sternbeck, A. Schiller and I. L. Bogolubsky, Braz. J. Phys. **37**, 193 (2007) [arXiv:hep-lat/0609043].

[52] A. Cucchieri, A. Maas and T. Mendes, Phys. Rev. D **77**, 094510 (2008) [arXiv:0803.1798 [hep-lat]].

[53] T. Kugo and I. Ojima, Prog. Theor. Phys. Suppl. **66**, 1 (1979) [Erratum Prog. Theor. Phys. **71**, 1121 (1984)]; T. Kugo, arXiv:hep-th/9511033.

[54] A. Sternbeck and L. von Smekal, arXiv:0811.4300 [hep-lat].

[55] T. D. Bakeev, E. M. Ilgenfritz, V. K. Mitrjushkin and M. Mueller-Preussker, Phys. Rev. D **69** (2004) 074507 [arXiv:hep-lat/0311041]; A. Sternbeck, E. M. Ilgenfritz and M. Muller-Preussker, Phys. Rev. D **73**, 014502 (2006) [arXiv:hep-lat/0510109].

[56] A. Maas, arXiv:0808.3047 [hep-lat].

[57] V. N. Gribov, Nucl. Phys. B **139**, 1 (1978).

[58] I. M. Singer, Commun. Math. Phys. **60** (1978) 7.

[59] H. Neuberger, Phys. Lett. B **183**, 337 (1987).

[60] L. von Smekal, D. Mehta, A. Sternbeck and A. G. Williams, PoS **LAT2007** (2007) 382 [arXiv:0710.2410 [hep-lat]]; L. von Smekal, A. Jorkowski, D. Mehta and A. Sternbeck, PoS C **ONFINEMENT8** (2008) 048 [arXiv:0812.2992 [hep-th]].

[61] P. van Baal, arXiv:hep-th/9711070; . Semenov-Tyan-Shanskii and V. Franke, Zap. Nauch. Sem. Leningrad. Otdeleniya Matematicheskogo Instituta im V. A. Stekolov, AN SSSR, Vol. 120 (1982), 159 (In English translation: New York, Plenum Press 1986); G. Dell'Antonio, D. Zwanziger, Proceedings of the NATO Advanced Workshop on Probabilistic Methods in Quantum Field Theory and Quantum Gravity, Cargese. New York, Plenum Press (1986), 21.

[62] M. Tissier and N. Wschebor, arXiv:0809.1880 [hep-th].

[63] M. Q. Huber, R. Alkofer, C. S. Fischer and K. Schwenzer, Phys. Lett. B **659** (2008) 434 [arXiv:0705.3809 [hep-ph]].

[64] J. M. Pawłowski, work in preparation.

[65] S. Nedelko and J. M. Pawłowski, work in preparation.

[66] C. S. Fischer, R. Alkofer, T. Dahm and P. Maris, Phys. Rev. D **70** (2004) 073007 [arXiv:hep-ph/0407104].

[67] J. S. Ball and T. W. Chiu, Phys. Rev. D **22**, 2550 (1980) [Erratum-ibid. D **23**, 3085 (1981)].

[68] U. Bar-Gadda, Nucl. Phys. B **163**, 312 (1980).

[69] C. S. Fischer, P. Watson and W. Cassing, Phys. Rev. D **72**, 094025 (2005) [arXiv:hep-ph/0509213].

[70] C. S. Fischer, PhD thesis, arXiv:hep-ph/0304233.

[71] D. Zwanziger, Phys. Lett. B **257**, 168 (1991); Nucl. Phys. B **364**, 127 (1991); Nucl. Phys. B **412**, 657 (1994); Phys. Rev. D **65**, 094039 (2002) [arXiv: hep-th/0109224].

[72] A. Cucchieri, A. Maas and T. Mendes, Phys. Rev. D **75** (2007) 076003 [arXiv:hep-lat/0702022].

[73] A. C. Kalloniatis, L. von Smekal and A. G. Williams, Phys. Lett. B **609** (2005) 424 [arXiv:hep-lat/0501016].

[74] L. von Smekal, M. Ghiotti and A. G. Williams, arXiv:0807.0480 [hep-th]; AIP Conf. Proc. **892** (2007) 180 [arXiv:hep-th/0611058].

[75] D. Zwanziger, Nucl. Phys. B **485** (1997) 185 [arXiv:hep-th/9603203]. See especially the statement following eq. (6.9) and Appendix C.

[76] C. S. Fischer, B. Grüter and R. Alkofer, Annals Phys. **321**, 1918 (2006) [arXiv:hep-ph/0506053].

[77] C. S. Fischer, A. Maas, J. M. Pawłowski and L. von Smekal, Annals Phys. **322** (2007) 2916 [arXiv:hep-ph/0701050].

[78] D. Zwanziger, Nucl. Phys. B **399** (1993) 477.

[79] J. A. Gracey, Phys. Lett. B **632** (2006) 282 [arXiv:hep-ph/0510151].

[80] A. Maas, J. Wambach and R. Alkofer, Eur. Phys. J. C **42** (2005) 93 [arXiv:hep-ph/0504019].

[81] P. O. Bowman, U. M. Heller, D. B. Leinweber, M. B. Parappilly and A. G. Williams, Phys. Rev. D **70**, 034509 (2004) [arXiv:hep-lat/0402032].

[82] A. Maas, J. Wambach, B. Grüter and R. Alkofer, Eur. Phys. J. C **37**, 335 (2004) [arXiv:hep-ph/0408074].

[83] R. Alkofer, C. S. Fischer, F. J. Llanes-Estrada and K. Schwenzer, arXiv:0804.3042 [hep-ph], accepted by Ann. Phys..

[84] A. Cucchieri, Nucl. Phys. B **521**, 365 (1998) [arXiv:hep-lat/9711024].

[85] H. Reinhardt and W. Schleifenbaum, arXiv:0809.1764 [hep-th].

[86] A. Cucchieri, T. Mendes, O. Oliveira and P. J. Silva, Phys. Rev. D **76** (2007) 114507 [arXiv:0705.3367 [hep-lat]].

[87] A. Sternbeck, L. von Smekal, D. B. Leinweber and A. G. Williams, PoS **LAT2007** (2007) 340 [arXiv:0710.1982 [hep-lat]].

[88] A. Maas, Mod. Phys. Lett. A **20**, 1797 (2005) [arXiv:hep-ph/0506066].

[89] A. Maas and Š. Olejník, JHEP **0802**, 070 (2008) [arXiv:0711.1451 [hep-lat]].

[90] R. Alkofer, W. Detmold, C. S. Fischer and P. Maris, Phys. Rev. D **70**, 014014 (2004) [arXiv:hep-ph/0309077].

[91] P. O. Bowman *et al.*, Phys. Rev. D **76**, 094505 (2007) [arXiv:hep-lat/0703022].

[92] A. Cucchieri, T. Mendes and A. R. Taurines, Phys. Rev. D **71**, 051902 (2005) [arXiv:hep-lat/0406020].

[93] N. K. Nielsen, Nucl. Phys. B **101**, 173 (1975).